

First Passage Time for Many Particle Diffusion in Space-Time Random Environments

Jacob B. Hass*, Ivan Corwin†, Eric I. Corwin*
*Department of Physics and Materials Science Institute,
University of Oregon, Eugene, Oregon 97403, USA.

†Department of Mathematics, Columbia University, New York, New York 10027, USA.
(Dated: August 3, 2023)

The first passage time for a single diffusing particle has been studied extensively, but the first passage time of a system of many diffusing particles, as is often the case in physical systems, has received little attention until recently. We consider two models for many particle diffusion – one treats each particle as independent simple random walkers while the other treats them as coupled to a common space-time random forcing field that biases particles nearby in space and time in similar ways. The first passage time of a single diffusing particle under both of these models show the same statistics and scaling behavior. However, for many particle diffusions, the first passage time among all particles (the ‘extreme first passage time’) is very different between the two models, effected in the latter case by the randomness of the common forcing field. We develop an asymptotic (in the number of particles and location where first passage is being probed) theoretical framework to separate out the impact of the random environment with that of sampling trajectories within it. We identify a new power-law describing the impact to the extreme first passage time variance of the environment. Through numerical simulations we verify that the predictions from this asymptotic theory hold even for systems with widely varying numbers of particles, all the way down to 100 particles. This shows that measurements of the extreme first passage time for many-particle diffusions provide an indirect measurement of the underlying environment in which the diffusion is occurring.

I. INTRODUCTION

The *extreme* (or fastest) first passage time beyond a barrier among many particles diffusing in a common environment determines the function of a variety of system such as oocyte fertilization [1–3], neuronal activation [4] and information flow in networks [5, 6]. When particles are modeled as independent simple symmetric random walks (SSRW) or Brownian motions [7–9], there has been extensive study of the first passage behavior for a single particle [10], or recently for many particles [1, 2, 11–17].

We probe the behavior of extreme first passage time for a model of many particle diffusion where particles are modeled as random walks in a common environment of space-time inhomogeneous biases which are, themselves, modeled by a random field with short-range correlations in space and time. We focus on this (time-dependent) random walk in random environment (RWRE) model in one spatial dimension as would be relevant to diffusion in long and thin capillaries. Self-averaging of the environment implies that the statistical behavior of a single (or typical) particle in the RWRE model remains unchanged compared to the SSRW model [18–20]. However, the extreme behavior of particles in the RWRE model has recently been shown to be quite different to that of the SSRW, with statistics and power-laws related to the Kardar-Parisi-Zhang (KPZ) universality class and equation [21–23] (see also [24–34]). Those works focus on the statistical behavior of the locations of the particles that move the furthest from a common starting position as a function of time and the number of particles, N . The location of the furthest particle is a complementary measurement to the extreme first passage time which measures time as a function of the location of a boundary.

Here we leverage the theoretical and asymptotic (in $N \rightarrow \infty$) results on extreme particle locations in the RWRE model [21, 22] to make precise finite N predictions about extreme first passage time statistics as a function of the location, L , of first passage and the number of particles, N . We show that the effect of the randomness of the environment and of sampling N random walks in that environment are approximately independent. This means that by probing the extreme first passage time we are able to gain access to certain measurements of the hidden environment in which the diffusion occurs. Using numerical simulations, we show that these predictions remain valid down to quite small systems of $N = 100$.

II. BACKGROUND

Classical modeling of diffusion [7–9] has served as a basis for the development of more complex models such as Lévy flights in biological systems [35], anomalous diffusion where the mean squared distance is not linear [36, 37], and active materials where particles have internal stores of energy [38, 39]. The aforementioned models modify the existing framework of classical diffusion to better model specific phenomenon, whereas we study a model that aims to better capture the behavior of classical diffusion in generality.

We consider a particular type of random walk in random environment (RWRE) models. RWRE models have been studied extensively and come in various forms, including those with short range correlated forces [40–44], long range correlated forces [37, 45–48] and only spatially varying random forces [45, 49–52]. We consider a short range, spatially and temporally varying random field.

Extreme first passage time statistics for classical mod-

els of many particle diffusion (e.g. N independent SS-RWs) have been studied extensively [1, 2, 11–17]. For RWRE models with a temporally constant environment [17, 53, 54] studied the aspects of first passage times for one and many particle diffusions. In our setting of a temporally varying environment, [26] (see the supplementary materials in [55]) initiated the study of extreme first passage time upon which we will expand.

III. MODEL FOR DIFFUSION

We consider independent random walks subject to a common environment which determines the bias at each site. We model the environment as independent and identically distributed (i.i.d.) transition biases $\mathbf{B} = \{B(x, t) : x \in \mathbb{Z}, t \in \mathbb{Z}_{\geq 0}\}$ drawn from a distribution supported on $[0, 1]$. In this work we focus on the *Random Walk in Random Environment (RWRE)* model where $B(x, t)$ are drawn from the uniform distribution on $[0, 1]$. If instead all $B(x, t) = 1/2$ our model reduces to the *Simple Symmetric Random Walk (SSRW)* model for diffusion. We write $\mathbb{P}(\bullet)$ for the probability of an event \bullet , and $\mathbb{E}[\bullet]$ and $\text{Var}(\bullet)$ for the expectation and variance of a random variable \bullet averaged over the random environment \mathbf{B} . For a given environment \mathbf{B} , we use that notation $\mathbb{P}^{\mathbf{B}}(\bullet)$, $\mathbb{E}^{\mathbf{B}}[\bullet]$ and $\text{Var}^{\mathbf{B}}(\bullet)$ to represent the probability of an event \bullet (in the first case) or random variable \bullet (in the second and third cases) given the environment \mathbf{B} . Recall the laws of total probability, expectation and variance

$$\begin{aligned} \mathbb{P}(\bullet) &= \mathbb{P}(\mathbb{P}^{\mathbf{B}}(\bullet)), & \mathbb{E}[\bullet] &= \mathbb{E}[\mathbb{E}^{\mathbf{B}}[\bullet]], \\ \text{Var}(\bullet) &= \text{Var}(\mathbb{E}^{\mathbf{B}}[\bullet]) + \mathbb{E}[\text{Var}^{\mathbf{B}}(\bullet)]. \end{aligned} \quad (1)$$

Let us describe now the motion of a single particle given the environment \mathbf{B} . We denote the position of a single particle at time $t \in \mathbb{Z}_{\geq 0}$ as $X(t) \in \mathbb{Z}$. It evolves as the following Markov chain. We begin at the origin such that $X(0) = 0$. Subsequently for all $t \in \mathbb{Z}_{\geq 0}$ if the particle is at position $X(t) = x$ it flips a weighted coin which has probability of heads $B(x, t)$ and tails $1 - B(x, t)$. If heads, the particle changes position such that $X(t+1) = X(t) + 1$ and if tails then $X(t+1) = X(t) - 1$. We use $p^{\mathbf{B}}(x, t) := \mathbb{P}^{\mathbf{B}}(X(t) = x)$ to denote the probability mass function for $X(t)$ which uniquely solves the Kolmogorov backwards equation

$$\begin{aligned} p^{\mathbf{B}}(x, t) &= p^{\mathbf{B}}(x-1, t-1)B(x-1, t-1) \\ &\quad + p^{\mathbf{B}}(x+1, t-1)(1-B(x+1, t-1)) \end{aligned}$$

for $x \in \mathbb{Z}$ and $t \in \mathbb{Z}_{\geq 0}$ with initial condition $p^{\mathbf{B}}(x, 0) = \mathbf{1}_{x=0}$ (with the notation $\mathbf{1}_E$ equals 1 if the event E occurs and 0 otherwise). For $L \in \mathbb{N}$ we define the (random) first passage time, τ_L , for $X(t)$ as

$$\tau_L = \min(t : X(t) \notin (-L, L)),$$

i.e., the time when the particle first exits $(-L, L)$.

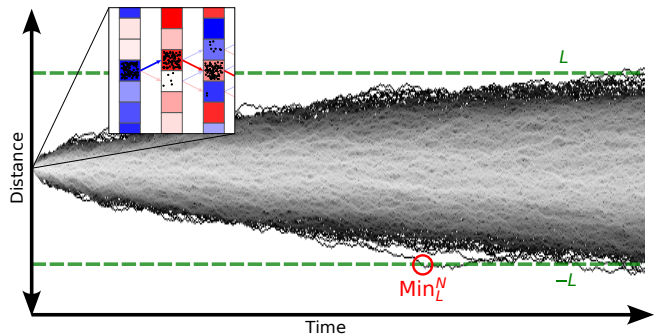


FIG. 1. A system of $N = 10^5$ particles evolving according to our RWRE model. The green dashed lines denote a barrier at $-L$ and L . The extreme first passage time, Min_L^N , is identified by the red circle and is the first time when one of these N walkers crosses this barrier. The inset illustrates the dynamics of particles in the first three time steps (not all 10^5 particles are shown to avoid cluttering). The color of each box in the inset corresponds to the bias of the location (blue means upward bias and red means downward bias).

We consider N particles $X^1(t), \dots, X^N(t)$ evolving independently in the same environment \mathbf{B} . This means that if multiple particles are at the same location and the same time, they use the same biased coins to determine their next move, though the flips of those coins are done independently of each other. For $i \in \{1, \dots, N\}$ let τ_L^i denote the first passage time for particle $X^i(t)$. Given the environment, the laws of $\tau_L^1, \dots, \tau_L^N$ are independent and identically distributed. We will study the first time *any* of the N particles leave $(-L, L)$ which we call the *extreme first passage time* and denote by $\text{Min}_L^N = \min(\tau_L^1, \dots, \tau_L^N)$. A visualization of our system and the extreme first passage time can be seen in Fig. 1.

The probability distribution of τ_L and consequently that of Min_L^N can be computed by studying $X_L(t) := X(\min(t, \tau_L))$, the random walk $X(t)$ stopped (or absorbed) when it first exits $(-L, L)$. The corresponding probability mass function $p_L^{\mathbf{B}}(x, t) := \mathbb{P}^{\mathbf{B}}(X_L(t) = x)$ uniquely solves the Kolmogorov backwards equation

$$\begin{aligned} p_L^{\mathbf{B}}(x, t) &= p_L^{\mathbf{B}}(x-1, t-1)B(x-1, t-1) \\ &\quad + p_L^{\mathbf{B}}(x+1, t-1)(1-B(x+1, t-1)) \end{aligned} \quad (2)$$

for $x \in [-L+2, L-2] \cap \mathbb{Z}$ and $t \in \mathbb{Z}_{\geq 0}$ subject absorbing boundary conditions whereby

$$\begin{aligned} p_L^{\mathbf{B}}(L, t) &= p_L^{\mathbf{B}}(L, t-1) \\ &\quad + B(L-1, t-1)p_L^{\mathbf{B}}(L-1, t-1), \\ p_L^{\mathbf{B}}(L-1, t) &= p_L^{\mathbf{B}}(L-2, t-1)B(L-2, t-1), \\ p_L^{\mathbf{B}}(-L+1, t) &= p_L^{\mathbf{B}}(-L+2, t-1)(1-B(-L+2, t-1)), \\ p_L^{\mathbf{B}}(-L, t) &= p_L^{\mathbf{B}}(-L, t-1) \\ &\quad + p_L^{\mathbf{B}}(-L+1, t-1)(1-B(-L+1, t-1)), \end{aligned} \quad (3)$$

and initial condition $p_L^{\mathbf{B}}(x, 0) = \mathbf{1}_{x=0}$. The probability of τ_L occurring before time t is the same as the probability of being absorbed before time t which is given by

$$\mathbb{P}^{\mathbf{B}}(\tau_L \leq t) = p_L^{\mathbf{B}}(L, t) + p_L^{\mathbf{B}}(-L, t). \quad (4)$$

From this, the probability distribution of the extreme first passage time Min_L^N is then given by

$$\mathbb{P}^{\mathbf{B}}(\text{Min}_L^N \leq t) = 1 - (1 - \mathbb{P}^{\mathbf{B}}(\tau_L \leq t))^N \quad (5)$$

since each τ_L^i is independent and identically distributed with probability distribution function $\mathbb{P}^{\mathbf{B}}(\tau_L \leq t)$.

There are two sources of randomness at play in Min_L^N . The first is due to the randomness of the underlying environment \mathbf{B} and the second due to sampling random walks in said environment. We seek to study the impact of each and their interplay. We define a natural proxy, Env_L^N , for the randomness due to the environment by

$$\text{Env}_L^N := \min \left(t : \mathbb{P}^{\mathbf{B}}(\tau_L \leq t) \geq \frac{1}{N} \right). \quad (6)$$

Notice that Env_L^N is deterministic given \mathbf{B} and, in light of Eq. 5, that it approximately satisfies $\mathbb{P}^{\mathbf{B}}(\text{Min}_L^N \leq \text{Env}_L^N) \approx 1 - (1 - 1/N)^N \approx e^{-1}$. The reason the first approximation is not an equality is because generally $\mathbb{P}^{\mathbf{B}}(\tau_L \leq t) \geq \frac{1}{N}$ in Eq. 6 will not strictly be equal to $1/N$. The difference

$$\text{Sam}_L^N := \text{Min}_L^N - \text{Env}_L^N, \quad (7)$$

which is still random given \mathbf{B} , contains the randomness from sampling $\tau_L^1, \dots, \tau_L^N$ given the environment \mathbf{B} .

While we have chosen to study the extreme first passage time of one or many particles leaving the region $(-L, L)$, we could just as well have studied the analogous time for leaving the region $(-\infty, L)$. The former case (studied mostly here) is the two-sided case while the latter is the one-sided case. The two-sided case benefits from the fact that $\mathbb{E}[\text{Min}_L^N] < \infty$ for all $N \geq 1$ while in the one-sided case, this mean is infinite for small enough N . Owing to this heavy-tailed nature of the one-sided case, it is numerically less efficient to study than in the two-sided case. On the other hand, our theoretical framework and asymptotic predictions provided below can be easily extended to the one-sided case. We will mostly focus on the two-sided case but also record some results for the one-sided case. Thus, in anticipation of that, let us define the first passage time $\tilde{\tau}_L = \min(t : X(t) < L)$ and the stopped random walk $\tilde{X}_L(t) := X(\min(t, \tilde{\tau}_L))$, whose probability mass function $\tilde{p}_L^{\mathbf{B}}(x, t) := \mathbb{P}^{\mathbf{B}}(\tilde{X}_L(t) = x)$ obeys the same equation and initial condition as the double sided case, but without the absorbing boundary at $-L$. Thus $\tilde{p}_L^{\mathbf{B}}(x, t)$ satisfies Eq. 2 for $x \in (-\infty, L-1) \cap \mathbb{Z}$ subject to the first two equalities in Eq. 3.

IV. NUMERICAL METHODS

In what follows we will study the mean and variance of $\text{Min}_L^N, \text{Env}_L^N$ and Sam_L^N . We will numerically measure the values of these quantities via methods described here, and to distinguish these numerical measurements from the true value, we will introduce a superscript so that $\mathbb{E}^{\text{Num}}[\bullet]$ and $\text{Var}^{\text{Num}}(\bullet)$ represent the numerically measured mean and variances of \bullet .

Given an environment \mathbf{B} , we can exactly sample the motion of N particles in it by following the agent-based definition whereby each particle evolves as a random walk with biases given by \mathbf{B} . When N is large it is not feasible to use the agent-based approach. Instead, as in [23], we obtain massive increase in efficiency by noting that if there are $N(x, t)$ particles at site x and time t , they will split into right and left moving populations according to a Binomial distribution. Specifically, the number of particles that move from site x at time t to site $x+1$ at time $t+1$ is drawn from a Binomial distribution with $N(x, t)$ trials and success probability $B(x, t)$. The remaining particles move to site $x-1$ at time $t+1$. This occupation variable based approach provides a way to exactly sample the number of particles per site over time which is sufficient to study the first passage times in question here.

In this work we present results on systems of $N = 10^2$ to $N = 10^{28}$ particles and measure the time of first passage for distances up to $L = 750 \cdot \ln(N)$. We measure the extreme first passage time past multiple distances in the same simulation by recording the time at which a particle first leaves each given boundary. We numerically measure $\mathbb{E}[\text{Min}_L^N]$ and $\text{Var}(\text{Min}_L^N)$ by choosing, according to the uniform distribution on each $B(x, t)$, an environment, \mathbf{B} , and then sampling Min_L^N as described above. Repeating this for many independently sampled environments allows us to build up the distribution of Min_L^N and thus estimate $\mathbb{E}[\text{Min}_L^N]$ and $\text{Var}(\text{Min}_L^N)$. For different values of N we repeat this procedure. However, for a given value of N , we make use of the same environment to study the statistics of Min_L^N for multiple values of L . Though this introduces some correlation in these numerically computed statistics at different distances, these should become negligible for a large sample size (i.e., the number of different instances of \mathbf{B} used).

To study Env_L^N , we compute $p_L^{\mathbf{B}}(x, t)$ for a given environment, \mathbf{B} , and distance L by numerically solving Eq. 2 with the boundary conditions Eq. 3 and initial condition $p_L^{\mathbf{B}}(x, 0) = \mathbf{1}_{x=0}$. From $p_L^{\mathbf{B}}(x, t)$ we calculate $\mathbb{P}^{\mathbf{B}}(\tau_L \leq t)$ using Eq. 4. We then measure Env_L^N for a given environment using its definition in Eq. 6. By computing $\mathbb{P}^{\mathbf{B}}(\tau_L \leq t)$ for many independent samples of the environment \mathbf{B} , we estimate $\mathbb{E}[\text{Env}_L^N]$ and $\text{Var}(\text{Env}_L^N)$.

We measure Sam_L^N using the following process. For a given environment \mathbf{B} , we calculate the probability distribution of Sam_L^N using Eq. 5 and 7, i.e.,

$$\mathbb{P}^{\mathbf{B}}(\text{Sam}_L^N \leq t) = 1 - (1 - \mathbb{P}^{\mathbf{B}}(\tau_L \leq t + \text{Env}_L^N))^N. \quad (8)$$

Using $\mathbb{P}^{\mathbf{B}}(\text{Sam}_L^N \leq t)$, we calculate $\mathbb{E}^{\mathbf{B}}[\text{Sam}_L^N]$ and $\text{Var}^{\mathbf{B}}[\text{Sam}_L^N]$ numerically. We are using the notation $\mathbb{E}^{\mathbf{B}}[\bullet]$ and $\text{Var}^{\mathbf{B}}[\bullet]$ introduced in Sec. III. We can then numerically measure $\mathbb{E}[\text{Sam}_L^N]$ and $\text{Var}[\text{Sam}_L^N]$ by sampling many independent instances of \mathbf{B} and using the laws of total expectation and variance in Eq. 1.

We probe four values of N , $N = 10^2, 10^5, 10^{12}$ and 10^{28} . To measure statistics involving Min_L^N we use 20,000, 10,000, 10,000 and 2,500 systems for the respective values of N , while to measure statistics involving Env_L^N and Sam_L^N we use 2,000, 2,000, 2,000 and 1,000 systems for the respective values of N . Notice that we used fewer systems for Env_L^N and Sam_L^N than for Min_L^N . This is because Min_L^N can be sampling via simulating the motion of N particles as described above while Env_L^N and Sam_L^N require computing the probability distribution by solving the master equation. The former is computationally much less expensive than the latter, hence our reduction in number of iterations. For measuring statistics involving Min_L^N for the SSRW model we use 5,000 systems (in other words, we repeatedly sampling N SSRWs and observe Min_L^N for a total of 5,000 instances).

To compute the data presented in this paper, we used 500 CPUs on a high performance computing cluster for approximately two weeks. Our code is available at <https://github.com/CorwinLab/RWRE-Simulations>.

V. DERIVATION OF ASYMPTOTIC PREDICTIONS

We derive asymptotic predictions for the extreme first passage time for the RWRE model in the limit where both L and N tending towards infinity with certain relationships. We study the mean and variances of Min_L^N , Env_L^N and Sam_L^N and develop asymptotic formulas that we subsequently compare to our numerical simulations in Sec. VI. We use the notation $\mathbb{E}^{\text{Asy}}[\bullet]$ and $\text{Var}^{\text{Asy}}(\bullet)$ to distinguish our formulas from the true values of $\mathbb{E}[\bullet]$ and $\text{Var}(\bullet)$ in question.

We find that there are three different scaling regimes with smooth transitions between them, consistent with previous results in [23] (which probes for different N the location of the maximum as a function of time, instead of the first passage times as a function of barrier location). The short distance regime is when $L/\ln(N) \rightarrow \hat{L} < 1$, in which case we will easily see that with very high probability at least one particle will move ballistically (hence resulting in trivial behaviors for the mean and variances in question). The medium distance regime is when $L/\ln(N) \rightarrow \hat{L} \in (1, \infty)$ in which case we leverage results from [21] to derive our asymptotic formulas related to the Gaussian Unitary Ensemble (GUE) Tracy-Widom (TW) distribution [56]. The large distance regime is when $L/(\ln(N))^{3/2} \rightarrow \hat{L} \in (0, \infty)$ in which case we leverage results from [22] to derive our asymptotic formulas related to the statistics of the solution to the

KPZ equation with narrow wedge initial data [57–61]. In each of these regimes we derive asymptotic approximations for the mean and variance of Sam_L^N and Env_L^N and argue they are independent when L and N tend towards infinity. Using this independence and these asymptotics for Sam_L^N and Env_L^N , we then likewise provide formulas for the asymptotic mean and variance of the extreme first passage time, Min_L^N , as recorded in Eqs. 38 and 39.

The study of extreme first passage time for the RWRE model was initiated in work of [26] (in particular, see the supplemental material in [55]) which focused on the fluctuations of Env_L^N in the medium distance regime. Our work in this section builds upon that analysis, offering some additional justification (based in part on KPZ scaling theory) and refinement as well as expanding to the large distance regime. We also develop the theory describing the sampling fluctuations Sam_L^N . In particular, we describe how the environmental and sampling fluctuations should be independent. Moreover, we propose a finite N formula based on stitching together these two asymptotic regimes. In the subsequent Section VI we verify our theory for a wide range of N through numerical simulations.

A. Short Distance Regime

We assume that $L, N \rightarrow \infty$ with $L/\ln(N) \rightarrow \hat{L} < 1$. In this case, it is very likely that at least one of the N particles will arrive at position $\pm L$ at time $t = L$ in which case we can conclude that $\mathbb{E}^{\text{Asy}}[\text{Min}_L^N] = L$ and $\text{Var}^{\text{Asy}}(\text{Min}_L^N) = 0$. Similarly, we see that $\mathbb{E}^{\text{Asy}}[\text{Env}_L^N] = L$ and $\text{Var}^{\text{Asy}}(\text{Env}_L^N) = \mathbb{E}^{\text{Asy}}[\text{Sam}_L^N] = \text{Var}^{\text{Asy}}(\text{Sam}_L^N) = 0$. To see this observe that the probability that a given particle will arrive at position $\pm L$ at time $t = L$ is given by

$$p^{\mathbf{B}}(L, L) + p^{\mathbf{B}}(-L, L) = \prod_{x=1}^L B(x, x) + \prod_{x=1}^{-L} (1 - B(x, -x))$$

where the $B(x, t)$ are i.i.d. uniform random variables. We use the law of large numbers to see that

$$\ln(p^{\mathbf{B}}(L, L)) = \sum_{x=1}^L \ln(B(x, x)) \approx -L$$

where we have used the fact that $-\ln(B(x, x))$ is an exponential mean 1 random variable. The same holds for $p^{\mathbf{B}}(-L, L)$ thus we see that

$$p^{\mathbf{B}}(L, L) + p^{\mathbf{B}}(-L, L) \approx 2e^{-L} \approx 2e^{-\hat{L}\ln(N)} \gg 1/N$$

where we have used that $L/\ln(N) \rightarrow \hat{L} < 1$. When $p^{\mathbf{B}}(L, L) + p^{\mathbf{B}}(-L, L) \gg 1/N$ (as above) it is likely that at least one of N independent particles is at $\pm L$. This implies the above claimed results when $\hat{L} < 1$.

One-sided case: In the one-sided barrier case the exact same analysis above goes through except only the $p^{\mathbf{B}}(L, L)$ term should be considered above.

B. Medium Distance Regime Env_L^N Behavior

The behavior in the medium and large distance regimes is considerably more complex. We first study the random variable Env_L^N in these regimes. Then, based on asymptotics derived for its mean and variance we determine asymptotic predictions for Sam_L^N and Min_L^N .

In the medium and large distance regime our analysis relies on results [21, 22] derived using tools from quantum integrable systems. We will review these results below. In essence they provide precise asymptotic information about the distribution of $\mathbb{P}^{\mathbf{B}}(X(t) \geq L)$ in various limits as t and L grow. This information is not equivalent to the knowledge of the first passage time distribution $\mathbb{P}^{\mathbf{B}}(\tau_L \leq t)$ that we seek to understand here. While the event $\{X(t) \geq L\}$ implies $\{\tau_L \leq t\}$, the opposite is not true. It is possible that a particle will pass the barrier at a time prior to t and then backtrack behind it at time t . However, as L approaches t the events become more and more equivalent since it is harder for a particle to exit $(-L, L)$ and then backtrack when L is large. For instance, when $L = t$ (the maximal possible value) the two events become equivalent. Based on this reasoning we make the following approximation that improves as L grows relative to t :

$$p_L^{\mathbf{B}}(L, t) \approx \mathbb{P}^{\mathbf{B}}(X(t) \geq L), \quad p_L^{\mathbf{B}}(-L, t) \approx \mathbb{P}^{\mathbf{B}}(X(t) \leq -L).$$

Recall that $p_L^{\mathbf{B}}(L, t)$ and $p_L^{\mathbf{B}}(-L, t)$ are the probabilities of absorption at L and $-L$ up to time t and their sum, as in Eq. 4, yields $\mathbb{P}^{\mathbf{B}}(\tau_L \leq t)$. Thus, we arrive at the starting approximation for our analysis:

$$\mathbb{P}^{\mathbf{B}}(\tau_L \leq t) \approx \mathbb{P}^{\mathbf{B}}(X(t) \geq L) + \mathbb{P}^{\mathbf{B}}(X(t) \leq -L). \quad (9)$$

In the medium distance regime we assume that $L, N \rightarrow \infty$ with $L/\ln(N) \rightarrow \hat{L} \in (1, \infty)$. The key input from [21] is as follows. Define the random variable $\chi_{x,t}$ by

$$\ln(\mathbb{P}^{\mathbf{B}}(X(t) \geq x)) = -tI\left(\frac{x}{t}\right) + t^{1/3}\sigma\left(\frac{x}{t}\right)\chi_{x,t} \quad (10)$$

where $x \in [0, t] \cap \mathbb{Z}$ and for $v \in [0, 1)$

$$I(v) = 1 - \sqrt{1 - v^2}, \quad \text{and} \quad \sigma(v)^3 = \frac{2I(v)^2}{1 - I(v)}.$$

Then [21] shows that for $v \in (0, 1)$, $\chi_{vt,t}$ converges as $t \rightarrow \infty$ in distribution to a GUE TW random variable. By symmetry the result of [21] also holds if in Eq. 10, $\ln(\mathbb{P}^{\mathbf{B}}(X(t) \geq x))$ is replaced by $\ln(\mathbb{P}^{\mathbf{B}}(X(t) \leq -x))$ and $\chi_{x,t}$ is replaced by $\chi_{-x,t}$. It should be noted that while [21] does not address the joint distribution of $\chi_{x,t}$ for different values of x and t , it is possible to make predictions based on grounds of KPZ universality [62, 63]. In particular, for any $v \in (-1, 0) \cup (0, 1)$ as $T \rightarrow \infty$, the space-time random process $(x, t) \mapsto \chi_{vtT+xT^{2/3}, tT}$ should converge to the KPZ fixed point [64], and the limiting processes for distinct v should be independent. Moreover, the local regularity of the KPZ fixed point is known which should

translate into estimates on the regularity of $\chi_{x,t}$. Some of this understanding will justify the approximations that follow involving how $\chi_{x,t}$ changes when t varies.

Combining Eq. 9 and Eq. 10 yields

$$\begin{aligned} \ln(\mathbb{P}^{\mathbf{B}}(\tau_L \leq t)) &\approx \\ &-tI\left(\frac{L}{t}\right) + \ln\left(e^{t^{1/3}\sigma\left(\frac{L}{t}\right)\chi_{L,t}} + e^{t^{1/3}\sigma\left(\frac{L}{t}\right)\chi_{-L,t}}\right) \end{aligned} \quad (11)$$

We seek to study the random variable Env_L^N which is defined by Eq. 6 and essentially is the t such that $\mathbb{P}^{\mathbf{B}}(\tau_L \leq t) = 1/N$ holds. This yields the following implicit equation for Env_L^N

$$\begin{aligned} -\ln(N) &\approx -\text{Env}_L^N \cdot I\left(\frac{L}{\text{Env}_L^N}\right) + \\ \ln\left(e^{(\text{Env}_L^N)^{1/3}\sigma\left(\frac{L}{\text{Env}_L^N}\right)\chi_{L, \text{Env}_L^N}} + e^{(\text{Env}_L^N)^{1/3}\sigma\left(\frac{L}{\text{Env}_L^N}\right)\chi_{-L, \text{Env}_L^N}}\right). \end{aligned} \quad (12)$$

We will solve this equation perturbatively. The first order solution neglects the second line in Eq. 12 and yields

$$\text{Env}_L^N \approx T_0 := \frac{(\ln(N))^2 + L^2}{2\ln(N)} \quad (13)$$

i.e., T_0 solves $\ln(N) = T_0 I\left(\frac{L}{T_0}\right)$. We now assume that $\text{Env}_L^N \approx T_0 + \delta$ with $\delta \ll T_0$ containing the randomness of Env_L^N . Substituting this into Eq. 12 we can find δ approximately by solving

$$\begin{aligned} -\ln(N) &\approx -(T_0 + \delta) \cdot I\left(\frac{L}{T_0 + \delta}\right) + \\ &\ln\left(e^{T_0^{1/3}\sigma\left(\frac{L}{T_0}\right)\chi_{L, T_0}} + e^{T_0^{1/3}\sigma\left(\frac{L}{T_0}\right)\chi_{-L, T_0}}\right) \\ &\approx -(T_0 + \delta) \cdot \left(I\left(\frac{L}{T_0}\right) + \delta\partial_t I\left(\frac{L}{t}\right)\Big|_{t=T_0}\right) + \\ &\ln\left(e^{T_0^{1/3}\sigma\left(\frac{L}{T_0}\right)\chi_{L, T_0}} + e^{T_0^{1/3}\sigma\left(\frac{L}{T_0}\right)\chi_{-L, T_0}}\right). \end{aligned} \quad (14)$$

In the first comparison we neglected the fact that under the perturbation to T_0 we should write $\chi_{L, T_0 + \delta}$ and $\chi_{-L, T_0 + \delta}$. This, however, is justified by the fact that while T_0 is of order $\ln(N)$, δ (as we will see below) is of order $(\ln(N))^{1/3}$. By the KPZ scaling theory mentioned earlier, this change in the time variable of the χ process should have a small impact which we neglect in our approximation. In the second comparison we utilized the Taylor expansion $I\left(\frac{L}{T_0 + \delta}\right) \approx I\left(\frac{L}{T_0}\right) + \delta\partial_t I\left(\frac{L}{t}\right)\Big|_{t=T_0}$. Since T_0 satisfies $-\ln(N) = -T_0 I\left(\frac{L}{T_0}\right)$ we can cancel terms and solve for δ in the resulting equation

$$\begin{aligned} 0 &\approx -\delta T_0 \partial_t I\left(\frac{L}{t}\right)\Big|_{t=T_0} - \delta I\left(\frac{L}{T_0}\right) - \delta^2 \partial_t I\left(\frac{L}{t}\right)\Big|_{t=T_0} + \\ &\ln\left(e^{T_0^{1/3}\sigma\left(\frac{L}{T_0}\right)\chi_{L, T_0}} + e^{T_0^{1/3}\sigma\left(\frac{L}{T_0}\right)\chi_{-L, T_0}}\right). \end{aligned}$$

Since L and T_0 are both of order $\ln(N)$, it follows from the chain rule that $\partial_t I\left(\frac{L}{t}\right)\Big|_{t=T_0}$ is of order $(\ln(N))^{-1}$. Since the final term above is of order $(\ln(N))^{1/3}$ the only

consistent scaling for δ is that it be of order $(\ln(N))^{1/3}$ as well in which case all terms are of that order except the term with δ^2 which decays like $(\ln(N))^{-1/3}$. Thus, neglecting that term we solve for δ and find

$$\delta \approx \frac{\ln\left(e^{T_0^{1/3}\sigma\left(\frac{L}{T_0}\right)\chi_{L,T_0}} + e^{T_0^{1/3}\sigma\left(\frac{L}{T_0}\right)\chi_{-L,T_0}}\right)}{I\left(\frac{L}{T_0}\right) + T_0\partial_t I\left(\frac{L}{t}\right)\Big|_{t=T_0}}. \quad (15)$$

Therefore, we have shown that

$$\text{Env}_L^N \approx T_0 + \frac{\ln\left(e^{T_0^{1/3}\sigma\left(\frac{L}{T_0}\right)\chi_{L,T_0}} + e^{T_0^{1/3}\sigma\left(\frac{L}{T_0}\right)\chi_{-L,T_0}}\right)}{I\left(\frac{L}{T_0}\right) + T_0\partial_t I\left(\frac{L}{t}\right)\Big|_{t=T_0}}. \quad (16)$$

The above conclusion is in agreement with Eq. 89 in [55] (in the one-sided barrier case). In particular, our Env_L^N random variable is essentially the same as $T_{\text{Hit}}(\ell)$ with our L and their ℓ having the same meaning. Our rate function I is the same as their λ , and our \hat{L} is equivalent to $1/\hat{\gamma}$ in their notation.

From Eq. 16 we may extract the following conclusion regarding the asymptotic behaviors for the mean and variance of Env_L^N in the medium distance regime:

$$\mathbb{E}^{\text{Asy}}[\text{Env}_L^N] \approx M_1(L, N) \text{ and } \text{Var}^{\text{Asy}}(\text{Env}_L^N) \approx V_1(L, N)$$

where M_1 and V_1 are defined as

$$M_1(L, N) := \frac{(\ln(N))^2 + L^2}{2\ln(N)}$$

$$V_1(L, N) := \frac{\text{Var}\left(\ln\left(e^{T_0^{1/3}\sigma\left(\frac{L}{T_0}\right)\chi_{L,T_0}} + e^{T_0^{1/3}\sigma\left(\frac{L}{T_0}\right)\chi_{-L,T_0}}\right)\right)}{\left(I\left(\frac{L}{T_0}\right) + T_0\partial_t I\left(\frac{L}{t}\right)\Big|_{t=T_0}\right)^2} \quad (17)$$

We have dropped the mean of δ (which is over order $(\ln(N))^{1/3}$) from M_1 and only retained the first order term T_0 . On the other hand, V_1 is precisely the variance of δ (as T_0 is deterministic). $V_1(L, N)$ contains the variance of a non-trivial combination of two random variables χ_{L,T_0} and χ_{-L,T_0} . To estimate this variance we replace both by independent GUE TW random variables χ and χ' (as justified by the above recorded result of [21] and KPZ scaling theory. Under that replacement, the variance in the numerator in V_1 is

$$\int_{\mathbb{R}^2} dx dy \left(\ln\left(e^{T_0^{1/3}\sigma\left(\frac{L}{T_0}\right)x} + e^{T_0^{1/3}\sigma\left(\frac{L}{T_0}\right)y}\right) \right)^2 p(x)p(y)$$

$$- \left(\int_{\mathbb{R}^2} dx dy \ln\left(e^{T_0^{1/3}\sigma\left(\frac{L}{T_0}\right)x} + e^{T_0^{1/3}\sigma\left(\frac{L}{T_0}\right)y}\right) p(x)p(y) \right)^2 \quad (18)$$

where $p(x)$ and $p(y)$ are the probability density of the GUE TW distribution. We numerically approximate the double integrals over the xy plane by integrating over the region $x, y \in [-10, 10]$ as is justified by the rapid decay of the density p . In fact, this integral can be approximated

in the limit of large N as follows. Observe that $T_0 = \ln(N)\frac{\hat{L}^2+1}{2}$ where we let $L = \hat{L}\ln(N)$. Thus

$$T_0^{1/3}\sigma\left(\frac{L}{T_0}\right) = (\ln(N))^{1/3}\left(\frac{\hat{L}^2+1}{2}\right)\sigma\left(\frac{2\hat{L}}{\hat{L}^2+1}\right).$$

For fixed \hat{L} this implies that the exponent diverges like $(\ln(N))^{1/3}$. Since

$$\ln(e^{rA} + e^{rB}) \approx r \max(A, B) \text{ as } r \rightarrow \infty, \quad (19)$$

it follows that the numerator in Eq. 17 is approximately (as $N \rightarrow \infty$) given by

$$\left(T_0^{1/3}\sigma\left(\frac{L}{T_0}\right)\right)^2 \text{Var}(\max(\chi, \chi')) \quad (20)$$

where χ and χ' are independent GUE TW random variables. This variance can be computed via numerical integration and this need only be done once (as opposed to for various values of N and L as above).

One-sided case: The same reasoning as in the two-sided case yields expressions for the mean and variance of Env_L^N . Namely, M_1 and V_1 from Eq. 17 are replaced now by \tilde{M}_1 and \tilde{V}_1 where $M_1 = \tilde{M}_1$ and

$$\tilde{V}_1(L, N) := \left(\frac{T_0^{1/3}\sigma\left(\frac{L}{T_0}\right)}{I\left(\frac{L}{T_0}\right) + T_0\partial_t I\left(\frac{L}{t}\right)\Big|_{t=T_0}} \right)^2 \text{Var}(\chi)$$

where χ is a GUE TW random variable such that $\text{Var}(\chi) \approx 0.813$. The simplification in \tilde{V}_1 comes from the fact that only the χ_{L,T_0} term is present in the one-sided case – thus rather than dealing with the variance of the ln of a sum of exponentials, the ln and exponential terms cancel and the simpler expression follows.

C. Large Distance Regime Env_L^N Behavior

In the large distance regime we assume that $L, N \rightarrow \infty$ with $L/(\ln(N))^{3/2} \rightarrow \hat{L} \in (0, \infty)$. The key input from [22] (see also Eq. (67) in the supplementary material in [26]) is as follows: For $v \in (0, \infty)$ and $x = vt^{3/4}$

$$\ln(\mathbb{P}^{\mathbf{B}}(X(t) \geq x)) \approx -\frac{x^2}{2t} - \frac{x^4}{12t^3} + \ln\left(\frac{x}{t}\right) + h\left(0, \frac{x^4}{t^3}\right) \quad (21)$$

where $h(y, s)$ denotes the random height at position y and time s of the narrow wedge solution to the Kardar-Parisi-Zhang (KPZ) equation

$$\partial_s h(y, s) = \frac{1}{2}\partial_y^2 h(y, s) + \frac{1}{2}(\partial_y h(y, s))^2 + \eta(y, s) \quad (22)$$

where $\eta(y, s)$ is space-time white noise [57–61]. By symmetry Eq. 21 will also hold with $\ln(\mathbb{P}^{\mathbf{B}}(X(t) \leq -x))$ and with an asymptotically independent fluctuation term $h'\left(0, \frac{x^4}{t^3}\right)$ that has the same law as h .

Similar to our analysis in the medium distance regime, combining Eq. 9 and Eq. 10 yields

$$\begin{aligned} \ln(\mathbb{P}^{\mathbf{B}}(\tau_L \leq t)) &\approx \\ &-\frac{L^2}{2t} - \frac{L^4}{12t^3} + \ln\left(\frac{L}{t}\right) + \ln\left(e^{h(0, \frac{L^4}{t^3})} + e^{h'(0, \frac{L^4}{t^3})}\right) \end{aligned} \quad (23)$$

Env_L^N is essentially t such that $\mathbb{P}^{\mathbf{B}}(\tau_L \leq t) = 1/N$ which yields the implicit equation for Env_L^N

$$\begin{aligned} -\ln(N) &\approx -\frac{L^2}{2\text{Env}_L^N} - \frac{L^4}{12(\text{Env}_L^N)^3} + \ln\left(\frac{L}{\text{Env}_L^N}\right) + \\ &\ln\left(e^{h(0, \frac{L^4}{(\text{Env}_L^N)^3})} + e^{h'(0, \frac{L^4}{(\text{Env}_L^N)^3})}\right) \end{aligned} \quad (24)$$

where h and h' are independent as above. The first term on the right-hand side is dominant and solving $\ln(N) = \frac{L^2}{2T_0}$ yields the first order behavior of $\text{Env}_L^N \approx T_0$ with

$$T_0 = \frac{L^2}{2\ln(N)}.$$

Under our scaling of L , this term is of order $(\ln(N))^2$ while the other deterministic terms on the right-hand side of Eq. 24 are either order 1 or $\ln(\ln(N))$. Thus, for the sake of the mean of Env_L^N , T_0 will suffice. To study its variance we write $\text{Env}_L^N = T_0 + \delta$ where $\delta \ll T_0$ contains the randomness of Env_L^N . Neglecting the lower order terms in Eq. 24 (the second and third terms on the right-hand side), Taylor expanding $-\frac{L^2}{2\text{Env}_L^N} = -\frac{L^2}{2(T_0 + \delta)} \approx -\frac{L^2}{2T_0} + \frac{L^2}{2T_0^2}\delta$, and substituting T_0 for Env_L^N in the h and h' expressions (as is again justified by the KPZ scaling theory), we arrive at an approximation for

$$\delta \approx \frac{2T_0^2}{L^2} \ln\left(e^{h(0, \frac{L^4}{T_0^3})} + e^{h'(0, \frac{L^4}{T_0^3})}\right).$$

From the above we may extract the following conclusion regarding the asymptotic behaviors for the mean and variance of Env_L^N in the large distance regime:

$$\mathbb{E}^{\text{Asy}}[\text{Env}_L^N] \approx M_2(L, N) \text{ and } \text{Var}^{\text{Asy}}(\text{Env}_L^N) \approx V_2(L, N)$$

where M_1 and V_1 are defined as

$$\begin{aligned} M_2(L, N) &:= \frac{L^2}{2\ln(N)} \\ V_2(L, N) &:= \frac{L^4 \text{Var}\left(\ln\left(e^{h(0, \frac{8(\ln(N))^3}{L^2})} + e^{h'(0, \frac{8(\ln(N))^3}{L^2})}\right)\right)}{4(\ln(N))^4} \end{aligned} \quad (25)$$

Notice that for $L = (\ln(N))^{3/2} \hat{L}$ (as in the large distance regime scaling) the KPZ equation time $\frac{8(\ln(N))^3}{L^2} = 8/\hat{L}^2$. Thus, the calculation of the variance in V_2 requires numerically integration using

the exact formula for the one-point distribution for the KPZ equation from [58–61]. This formula is non-trivial to compute numerically due to its complexity. However, [65] (used in the work of [66]) contains the numerics for the density of $h(0, s)$ for $s \in \{0.25, 0.35, 0.5, 0.75, 1.2, 2, 3.5, 6.5, 13, 25, 50, 100, 250\}$. In the limit where $s \rightarrow 0$ or $s \rightarrow \infty$ the law of $h(0, s)$ converges to be Gaussian or GUE TW (with appropriate scaling) and thus we can combine these limiting behaviors with the numerical data to produce, via smooth interpolation, a curve

$$s \mapsto \text{Var}\left(\ln\left(e^{h(0, s)} + e^{h'(0, s)}\right)\right)$$

for all s that we use to numerically evaluate $V_2(L, N)$.

One-sided case: The same reasoning as in the two-sided case yields expressions for the mean and variance of Env_L^N . Namely, M_2 and V_2 from Eq. 25 are replaced now by \tilde{M}_2 and \tilde{V}_2 where $\tilde{M}_2 = M_2$ and

$$\tilde{V}_2(L, N) := \frac{L^4 \text{Var}\left(h(0, \frac{8(\ln(N))^3}{L^2})\right)}{4(\ln(N))^4}.$$

In this case, the variance in question was numerically computed and plotted in [66].

D. Stitching Together the Medium and Large Distance Regime Env_L^N Behavior

We compare the large L (in the $\ln(N)$ scale) behavior of $V_1(L, N)$ to the small L (in the $(\ln(N))^{3/2}$ scale) behavior of $V_2(L, N)$ and show that they match. This justifies defining $\text{Var}^{\text{Asy}}(\text{Env}_L^N)$ via smoothly stitching these two functions between these two scaling regimes. We then record the very large distance asymptotics that should persist for all L beyond the $(\ln(N))^{3/2}$ regime. We only address the variances below since $M_1(L, N)$ clearly converges to $M_2(L, N)$ when $L \gg \ln(N)$.

Recall $V_1(L, N)$ from Eq. 17. Using the discussion after Eq. 18, namely Eq. 20, we can approximate this as

$$V_1(L, N) \approx \frac{\left(T_0^{1/3} \sigma\left(\frac{L}{T_0}\right)\right)^2 \text{Var}(\max(\chi, \chi'))}{\left(I\left(\frac{L}{T_0}\right) + T_0 \partial_t I\left(\frac{L}{t}\right)\Big|_{t=T_0}\right)^2},$$

where χ and χ' are independent GUE TW random variables. Observe the following asymptotic: For $v \rightarrow 0$, $\sigma(v) \approx \frac{v^{4/3}}{2^{1/3}}$ while for $L \gg \ln(N)$, $T_0 \approx \frac{L^2}{2\ln(N)}$ and

$$I\left(\frac{L}{T_0}\right) + T_0 \partial_t I\left(\frac{L}{t}\right)\Big|_{t=T_0} \approx -2 \left(\frac{\ln(N)}{L}\right)^2.$$

Putting these together shows that for $L \gg \ln(N)$,

$$V_1(L, N) \approx \frac{L^{8/3} \text{Var}(\max(\chi, \chi'))}{2^{1/3} (\ln(N))^2}.$$

Now, let us compare this to the behavior of $V_2(L, N)$ from Eq. 25 when $L \ll (\ln(N))^{3/2}$. Observe that the KPZ equation time s in V_2 is given by $s = \frac{8(\ln(N))^3}{L^2}$ which goes to infinity as the ratio $L/(\ln(N))^{3/2}$ tends to zero. Thus, to extract the behavior of V_2 we must use the large time behavior of KPZ equation one-point distribution which says that the random variable χ_s defined by

$$h(0, s) \approx \chi \left(\frac{s}{2} \right)^{1/3} - \frac{s}{24},$$

converges as $s \rightarrow \infty$ to a GUE TW random variable [58–61]. Letting χ and χ' denote the limiting independent GUE TW random variables arising from h and h' in V_2 , and using Eq. 19, it follows that when $L \ll (\ln(N))^{3/2}$,

$$V_2(L, N) \approx \frac{L^{8/3} \text{Var}(\max(\chi, \chi'))}{2^{1/3} (\ln(N))^2}$$

which matches the $L \gg \ln(N)$ behavior of $V_1(L, N)$.

This matching of the two expressions V_1 and V_2 justifies stitching them together to provide a single continuous curve for the asymptotic variance of the environmental fluctuations Env_L^N . To do this we use an error function centered at $L = (\ln(N))^{5/4}$ with a width of $(\ln(N))^{6/5}$ to ensure a smooth crossover between the two regimes. The resulting asymptotic variance formula is then given by

$$\text{Var}^{\text{Asy}}(\text{Env}_L^N) = \phi(L, N) V_1(L, N) + (1 - \phi(L, N)) V_2(L, N) \quad (26)$$

where $V_1(L, N)$ and $V_2(L, N)$ are defined in Eqs. 17 and 25 respectively, where the interpolation function

$$\phi(L, N) := \frac{1}{2} \left(1 - \text{erf} \left(\frac{L - (\ln(N))^{5/4}}{(\ln(N))^{6/5}} \right) \right) \quad (27)$$

with the error function $\text{erf}(x) = \frac{2}{\sqrt{\pi}} \int_0^x e^{-y^2} dy$. We likewise define $\mathbb{E}^{\text{Asy}}[\text{Env}_L^N]$ via the same interpolation scheme as in Eq. 26 using the fact that M_1 and M_2 smoothly crossover too. In fact, since the large L asymptotic of M_1 is precisely in agreement with M_2 , the interpolation is essentially unnecessary.

The above asymptotic formula $\text{Var}^{\text{Asy}}(\text{Env}_L^N)$ will be compared to numerical simulations for wide ranges of N and L in Section VI. As will become clear there, the crossover $L^{8/3}/(\ln(N))^2$ power-law behavior observed above is something of a ghost. For realistic sizes of N the range between $\ln(N)$ and $(\ln(N))^{3/2}$ is rather narrow. For instance, in Section VI we study the range $N = 10^2$ to $N = 10^{28}$. On the lower end of this range, $\ln(N) \approx 4.6$ and $(\ln(N))^{3/2} \approx 9.9$ while on the upper end $\ln(N) \approx 64$ while $(\ln(N))^{3/2} \approx 517$. So, even for $N = 10^{28}$, there is not even a decade between $\ln(N)$ and $(\ln(N))^{3/2}$.

What is more important in terms of comparison to numerical data is the behavior of the variance of Env_L^N in the limit where $L \gg (\ln(N))^{3/2}$. This unbounded regime demonstrates a novel power-law that will be important to compare to the impact of the Sam_L^N variance.

To probe the behavior of $\text{Var}^{\text{Asy}}(\text{Env}_L^N)$ as $L \gg (\ln(N))^{3/2}$ we need only study the corresponding behavior of $V_2(L, N)$. In that case the KPZ time $s = \frac{8(\ln(N))^3}{L^2}$ goes to zero. Thus, we must make use of the small time (Edwards-Wilkinson) asymptotics that show that the random variable G_s defined by

$$h(0, s) \approx -\frac{s}{24} - \ln(\sqrt{2\pi s}) + \left(\frac{\pi s}{4} \right)^{1/4} G_s \quad (28)$$

converges as $s \rightarrow 0$ to a standard Gaussian random variable G [58–61]. Therefore, using $e^x \approx 1 + x$ and $\ln(1 + x) \approx x$ as $x \rightarrow 0$, we find that

$$\ln(e^{h(0,s)} + e^{h'(0,s)}) \approx -\frac{s}{24} - \ln\left(\sqrt{\frac{\pi s}{2}}\right) + \frac{1}{2} \left(\frac{\pi s}{4}\right)^{1/4} (G + G'). \quad (29)$$

Substituting $s = \frac{8(\ln(N))^3}{L^2}$ and taking the variance yields

$$\text{Var}\left(\ln\left(e^{h\left(0, \frac{8(\ln(N))^3}{L^2}\right)} + e^{h'\left(0, \frac{8(\ln(N))^3}{L^2}\right)}\right)\right) \approx \frac{1}{2} \left(\frac{2\pi(\ln(N))^3}{L^2}\right)^{1/2},$$

where we used that $\text{Var}(G + G') = 2$ since G and G' are independent standard Gaussian random variables. Substituting this into Eq. 25 shows that where $L \gg (\ln(N))^{3/2}$

$$\text{Var}^{\text{Asy}}(\text{Env}_L^N) \approx V_2(L, N) \approx \frac{1}{4} \sqrt{\frac{\pi}{2}} \frac{L^3}{(\ln(N))^{5/2}}. \quad (30)$$

This power-law behavior will be quite visible in the numerical data from Section VI.

One-sided case: The only difference in this case is that we use \tilde{V}_1 and \tilde{V}_2 in place of V_1 and V_2 . This crossover behavior between the regime where L is of order $\ln(N)$ and $(\ln(N))^{3/2}$ still matches up and the same interpolation formula Eq. 26 can be used. For the $L \gg (\ln(N))^{3/2}$ asymptotics, the right-hand side of Eq. 30 ends up being twice as large in the one-sided case as in the two-sided case. This may seem counter-intuitive since there are two Gaussians in the two-sided case versus one in the one-sided case. However, in the calculation in Eq. 29, we used $\ln(e^{h(0,s)} + e^{h'(0,s)}) \approx \ln(2) + \frac{1}{2}(h(0,s) + h'(0,s))$. The variance of $\frac{1}{2}(h(0,s) + h'(0,s))$ is half that of the variance of $h(0,s)$, thus explaining the factor of 2 difference.

E. Sam_L^N and Min_L^N Behavior

We now argue that the environmental and sampling fluctuations Env_L^N and Sam_L^N are independent and that the sampling fluctuations are Gumbel distributed. The independence is strongly supported by our numerical data, see for instance Figure 7.

To start, observe that for large N and small $\mathbb{P}^{\text{B}}(\tau_L \leq t)$ we can rewrite Eq. 5 as

$$\mathbb{P}^{\text{B}}(\text{Min}_L^N \geq t) \approx e^{-N\mathbb{P}^{\text{B}}(\tau_L \leq t)}. \quad (31)$$

Using the non-backtracking approximation in Eq. 9 and the medium distance range asymptotic expansion Eq. 10 we arrive at the starting formula

$$\ln(\mathbb{P}^{\mathbf{B}}(\text{Min}_L^N \geq t)) \approx -N \left(e^{-tI\left(\frac{L}{t}\right) + t^{1/3}\sigma\left(\frac{L}{t}\right)\chi_{L,t}} + e^{-tI\left(\frac{L}{t}\right) + t^{1/3}\sigma\left(\frac{L}{t}\right)\chi_{-L,t}} \right) \quad (32)$$

We will work here with in the medium distance regime asymptotics. A similar analysis could be performed in the large distance regime and the result would agree with the $L \gg \ln(N)$ behavior derived below so we do not repeat this derivation.

Recalling that $\text{Sam}_L^N = \text{Min}_L^N - \text{Env}_L^N$, we have that $\mathbb{P}^{\mathbf{B}}(\text{Sam}_L^N \geq s) = \mathbb{P}^{\mathbf{B}}(\text{Min}_L^N \geq \text{Env}_L^N + s)$. Thus we have that $\ln(\mathbb{P}^{\mathbf{B}}(\text{Sam}_L^N \geq s))$ is approximately given by the right-hand side of Eq. 32 with $t = \text{Env}_L^N + s$. With this in mind, we will use the following Taylor expansion in the exponential on the right-hand side of Eq. 32:

$$\begin{aligned} & -(\text{Env}_L^N + s)I\left(\frac{L}{\text{Env}_L^N + s}\right) \\ & + (\text{Env}_L^N + s)^{1/3}\sigma\left(\frac{L}{\text{Env}_L^N + s}\right)\chi_{L, \text{Env}_L^N + s} \approx \\ & -(\text{Env}_L^N + s)\left(I\left(\frac{L}{\text{Env}_L^N}\right) + s\partial_t I\left(\frac{L}{t}\right)\Big|_{t=\text{Env}_L^N}\right) \\ & + (\text{Env}_L^N)^{1/3}\sigma\left(\frac{L}{\text{Env}_L^N}\right)\chi_{L, \text{Env}_L^N} \approx \\ & \ln(\mathbb{P}^{\mathbf{B}}(X(\text{Env}_L^N) \geq L)) - \\ & s\left(I\left(\frac{L}{\text{Env}_L^N}\right) + \text{Env}_L^N\partial_t I\left(\frac{L}{t}\right)\Big|_{t=\text{Env}_L^N}\right) \end{aligned} \quad (33)$$

Notice that in the first comparison above we have assumed that $(\text{Env}_L^N + s)^{1/3}\sigma\left(\frac{L}{\text{Env}_L^N + s}\right)\chi_{L, \text{Env}_L^N + s}$ can be replaced by the same term with Env_L^N instead of $\text{Env}_L^N + s$. This is a non-trivial assumption which ultimately implies the Gumbel form of Sam_L^N and its independence from Env_L^N . This should be justifiable based on the KPZ scaling theory and the fact that (as we will see) $\mathbb{E}^{\text{Asy}}[\text{Env}_L^N] \gg \mathbb{E}^{\text{Asy}}[\text{Sam}_L^N]$. The second comparison uses Eq. 10 and throws out the s^2 term. Of course, the same expansion above applies when $L \mapsto -L$ and $\mathbb{P}^{\mathbf{B}}(X(\text{Env}_L^N) \geq L)$ is replaced by $\mathbb{P}^{\mathbf{B}}(X(\text{Env}_L^N) \leq -L)$. Putting these expansions together with Eq. 32 yields

$$\begin{aligned} & \ln(\mathbb{P}^{\mathbf{B}}(\text{Sam}_L^N \geq s)) \approx \\ & -N(\mathbb{P}^{\mathbf{B}}(X(\text{Env}_L^N) \geq L) + \mathbb{P}^{\mathbf{B}}(X(\text{Env}_L^N) \leq -L)) \\ & \times e^{-s\left(I\left(\frac{L}{\text{Env}_L^N}\right) + \text{Env}_L^N\partial_t I\left(\frac{L}{t}\right)\Big|_{t=\text{Env}_L^N}\right)} \end{aligned} \quad (34)$$

Invoking the non-backtracking approximation in Eq. 9 and the definition Eq. 6 of Env_L^N , it follows that $\mathbb{P}^{\mathbf{B}}(X(\text{Env}_L^N) \geq L) + \mathbb{P}^{\mathbf{B}}(X(\text{Env}_L^N) \leq -L) \approx \mathbb{P}^{\mathbf{B}}(\tau_L \leq \text{Env}_L^N) \approx 1/N$. Using this along with replacing Env_L^N by T_0 as in Eq. 13, from Eq. 34 we see that

$$\ln(\mathbb{P}^{\mathbf{B}}(\text{Sam}_L^N \geq s)) \approx -e^{-s\left(I\left(\frac{L}{T_0}\right) + T_0\partial_t I\left(\frac{L}{t}\right)\Big|_{t=T_0}\right)}.$$

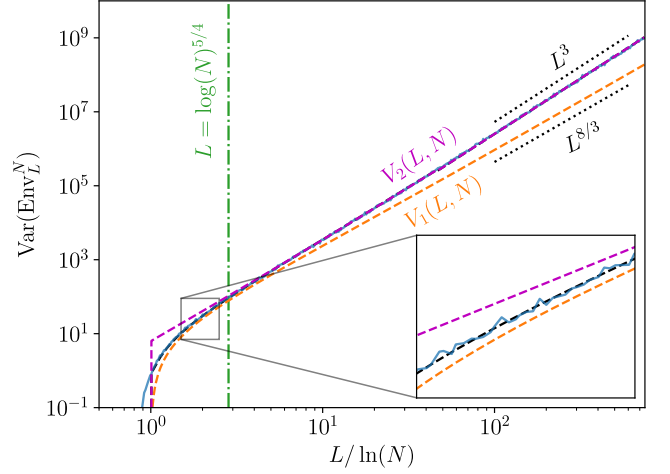


FIG. 2. We plot the environmental variance, $\text{Var}^{\text{Num}}(\text{Env}_L^N)$, for $N = 10^{28}$ particles (blue); the asymptotic variance V_1 for the short time regime given in Eq. 17 (orange dashed line); the asymptotic variance V_2 for the long time regime given in Eq. 25 (purple dashed line); the interpolation $\text{Var}^{\text{Asy}}(\text{Env}_L^N)$ between these regimes using Eq. 26 (black dashed line); and the power-law asymptotics of V_1 and V_2 (black dotted lines).

Observe that

$$\begin{aligned} I\left(\frac{L}{T_0}\right) + T_0\partial_t I\left(\frac{L}{t}\right)\Big|_{t=T_0} &= I(v) - vI'(v)\Big|_{v=L/T_0} \\ &= \frac{\sqrt{1-v^2}-1}{\sqrt{1-v^2}}\Big|_{v=L/T_0}, \end{aligned}$$

which is negative and behaves like $-v^2/2$ as $v \rightarrow 0$. This shows that asymptotically $-\text{Sam}_L^N$ has the law of a Gumbel distribution with location parameter 0 and scale parameter $-\left(I\left(\frac{L}{T_0}\right) + T_0\partial_t I\left(\frac{L}{t}\right)\Big|_{t=T_0}\right)^{-1}$. From this and the formula for the mean and variance of a Gumbel random variable in terms of its location and scale parameter we see that in the medium distance regime

$$\begin{aligned} \mathbb{E}^{\text{Asy}}[\text{Sam}_L^N] &\approx \frac{\gamma}{\left(I\left(\frac{L}{T_0}\right) + T_0\partial_t I\left(\frac{L}{t}\right)\Big|_{t=T_0}\right)}, \\ \text{Var}^{\text{Asy}}(\text{Sam}_L^N) &\approx \frac{\pi^2}{6\left(I\left(\frac{L}{T_0}\right) + T_0\partial_t I\left(\frac{L}{t}\right)\Big|_{t=T_0}\right)^2}, \end{aligned} \quad (35)$$

where $\gamma \approx .577$ is the Euler gamma constant. In the limit where $L \gg \ln(N)$ this yields

$$\begin{aligned} \mathbb{E}^{\text{Asy}}[\text{Sam}_L^N] &\approx -\frac{\gamma L^2}{2(\ln(N))^2}, \\ \text{Var}^{\text{Asy}}(\text{Sam}_L^N) &\approx \frac{\pi^2 L^4}{24(\ln(N))^4}. \end{aligned} \quad (36)$$

Observe that $\mathbb{E}^{\text{Asy}}[\text{Sam}_L^N] \ll \mathbb{E}^{\text{Asy}}[\text{Env}_L^N]$ since the former grows like $L^2/(\ln(N))^2$ while the latter

like $L^2/\ln(N)$. Thus, we are justified in dropping $\mathbb{E}^{\text{Asy}}[\text{Sam}_L^N]$ and approximating $\mathbb{E}^{\text{Asy}}[\text{Min}_L^N] \approx \mathbb{E}^{\text{Asy}}[\text{Env}_L^N]$ as we will do in Eq. 39.

Though the above derivation was done in the medium distance regime, the same could be repeated in the large distance regime and the above asymptotic behavior in Eq. 36 would follow (along with the Gumbel scaling limit for Sam_L^N). We do not repeat this calculation here. This, however, justifies using the asymptotic formula from Eq. 35 for both the medium and large distance regimes (and $L \gg (\ln(N))^{3/2}$ too).

From the above explained Gumbel limit, observe that the location and scale parameters are independent of Env_L^N and rather only depend on the first order behavior of Env_L^N given by T_0 . This implies the asymptotic independence and hence allows us to represent Min_L^N as a sum of Env_L^N (whose limiting distribution, mean and variance were identified earlier) and Sam_L^N (which is Gumbel distributed as above). This independence implies the following *addition law*

$$\text{Var}^{\text{Asy}}(\text{Min}_L^N) = \text{Var}^{\text{Asy}}(\text{Env}_L^N) + \text{Var}^{\text{Asy}}(\text{Sam}_L^N). \quad (37)$$

The same trivially holds for the mean.

Therefore, combining Eq. 26 with Eq. 35 we conclude (see also Figure 2)

$$\begin{aligned} \text{Var}^{\text{Asy}}(\text{Min}_L^N) \approx & \phi(L, N)V_1(L, N) + (1 - \phi(L, N))V_2(L, N) \\ & + \frac{\pi^2}{6 \left(I\left(\frac{L}{T_0}\right) + T_0 \partial_t I\left(\frac{L}{t}\right)\bigg|_{t=T_0} \right)^2} \end{aligned} \quad (38)$$

where $V_1(L, N)$ and $V_2(L, N)$ are defined in Eqs. 17 and 25 respectively, the interpolation function ϕ is defined in Eq. 27 and the final term comes from Eq. 35. Similarly,

$$\mathbb{E}^{\text{Asy}}[\text{Min}_L^N] \approx M_1(L, N). \quad (39)$$

It is worth emphasizing (and will be apparent in the numerical simulation data that follows) that in the asymptotic formula $\text{Var}^{\text{Asy}}(\text{Min}_L^N)$ in Eq. 38, there is a competition between $\text{Var}^{\text{Asy}}(\text{Env}_L^N)$ and $\text{Var}^{\text{Asy}}(\text{Sam}_L^N)$. By Eq. 30 $\text{Var}^{\text{Asy}}(\text{Env}_L^N)$ behaves (anywhere past the short lived medium distance regime) according to the power-law $L^3/(\ln(N))^{5/2}$ while by Eq. 36 $\text{Var}^{\text{Asy}}(\text{Sam}_L^N)$ likewise behaves like $L^4/(\ln(N))^{3/2}$. Setting these equal shows a crossover when L is of order $(\ln(N))^{3/2}$, i.e., the large distance regime. For smaller L , $\text{Var}^{\text{Asy}}(\text{Env}_L^N) \gg \text{Var}^{\text{Asy}}(\text{Sam}_L^N)$ while for larger L the opposite holds.

One-sided case: The behavior of Sam_L^N is easily seen to be asymptotically the same in this case. The behavior of Min_L^N thus involves combining the one-sided behavior of Env_L^N described earlier with the above behavior of Sam_L^N .

F. Asymptotic Behavior for the SSRW

We now derive the extreme first passage time behavior for the SSRW model where the transition biases are deterministic with $B(x, t) = 1/2$. We derive these results using the same techniques and assumptions used for the RWRE model. The methods used in [10, 13] should also yield an alternative derivation of the asymptotics below though we do not pursue that here. To distinguish from the RWRE model, we will use a tilde to label random variables and functions associated to the SSRW model below.

Just as for the RWRE model, we find a trivial short distance behavior for the SSRW model but with a larger cutoff on the short distance length scale. Namely, when $L, N \rightarrow \infty$ with $L/\ln(N) \rightarrow \tilde{L} < 1/\ln(2)$ the mean and variance of the extreme first passage time behaves asymptotically like $\mathbb{E}^{\text{Asy}}[\widetilde{\text{Min}}_L^N] \approx L$ and $\text{Var}^{\text{Asy}}(\widetilde{\text{Min}}_L^N) \approx 0$. The $1/\ln(2)$ comes from solving for L such that $(1/2)^L \approx 1/N$ (we do not need to use the law of large numbers here since all $B(x, t) = 1/2$).

The other length regime is when $L, N \rightarrow \infty$ with $L/\ln(N) \rightarrow \tilde{L} > 1/\ln(2)$ (or when $L/\ln(N)$ goes to infinity). Using Stirling's formula (or more generally Cramer's theorem from the large deviation theory) the tail of the probability distribution for the location of a SSRW $\tilde{X}(t)$ satisfies

$$\mathbb{P}(\tilde{X}(t) \geq x) \approx e^{-t\tilde{I}\left(\frac{x}{t}\right)} \quad (40)$$

where $\tilde{I}(v) = \frac{1}{2}((1+v)\ln(1+v) + (1-v)\ln(1-v))$ and where we no longer write $\mathbb{P}^{\mathbf{B}}$ since deterministically we have assumed here that all $B(x, t) = 1/2$.

Using the same non-backtracking approximation as in the RWRE case (Eq. 9) in conjunction with Eq. 40 yields

$$\mathbb{P}(\widetilde{\tau}_L \leq t) \approx 2e^{-t\tilde{I}\left(\frac{L}{t}\right)}. \quad (41)$$

We look for \tilde{T}_0 such that $\mathbb{P}(\widetilde{\tau}_L \leq \tilde{T}_0) = 1/N$. This is a deterministic analog to Env_L^N and plays the role of the centering of the extreme first passage time. Since \tilde{T}_0 is deterministic for the SSRW, there are no environmental fluctuations. Dropping the factor of 2 in Eq. 41 (as it is insignificant in the asymptotic regimes we consider here) \tilde{T}_0 should satisfy

$$\ln(N) \approx \tilde{T}_0 \cdot \tilde{I}\left(\frac{L}{\tilde{T}_0}\right). \quad (42)$$

Although we cannot solve this analytically for \tilde{T}_0 , we can solve for \tilde{T}_0 numerically and asymptotically in the limit $\tilde{T}_0 \rightarrow \infty$ (which occurs when L grows fast enough compared to $\ln(N)$) as we show below.

Substituting Eq. 41 into Eq. 31 and expanding about \tilde{T}_0 such that $\widetilde{\text{Min}}_L^N = \tilde{T}_0 + s$ yields

$$\mathbb{P}(\widetilde{\text{Min}}_L^N \geq \tilde{T}_0 + s) \approx e^{-2Ne^{-(\tilde{T}_0+s)\tilde{I}\left(\frac{L}{\tilde{T}_0+s}\right)}}.$$

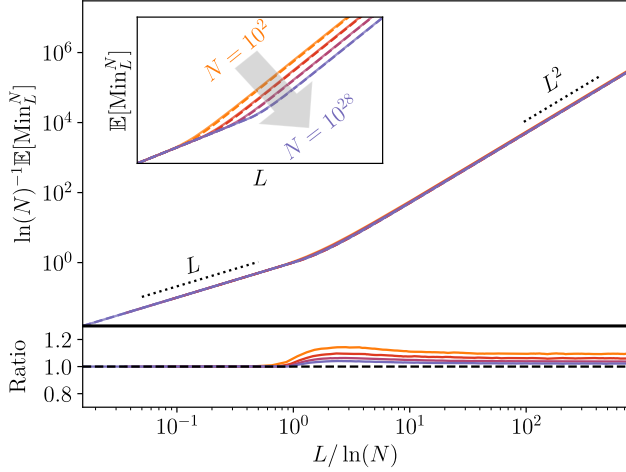


FIG. 3. We plot the mean of the extreme first passage time, $\mathbb{E}^{\text{Num}}[\text{Min}_L^N]$, using solid lines of varying colors for $N = 10^2, 10^5, 10^{12}$ and 10^{28} particles. The dashed lines are the asymptotic curves $\mathbb{E}^{\text{Asy}}[\text{Min}_L^N]$ from Eq. 39. The inset shows the uncollapsed data to better distinguish different values of N . The collapse occurs by scaling both the x -axis and y -axis by $\ln(N)$. The lower plot shows the ratio of $\mathbb{E}^{\text{Num}}[\text{Min}_L^N] / \mathbb{E}^{\text{Asy}}[\text{Min}_L^N]$ confirming the close fit.

Expanding about \tilde{T}_0 such that $\tilde{I}\left(\frac{L}{\tilde{T}_0+s}\right) \approx \tilde{I}\left(\frac{L}{\tilde{T}_0}\right) + s\partial_t \tilde{I}\left(\frac{L}{t}\right)\Big|_{t=\tilde{T}_0}$ gives

$$\mathbb{P}(\widetilde{\text{Min}}_L^N \geq \tilde{T}_0 + s) \approx e^{-e^{-s\left(\tilde{I}\left(\frac{L}{\tilde{T}_0}\right) + \tilde{T}_0\partial_t \tilde{I}\left(\frac{L}{t}\right)\Big|_{t=\tilde{T}_0}\right)}}$$

This shows $-\widetilde{\text{Min}}_L^N$ is Gumbel distributed with location parameter $-\tilde{T}_0$ and scale parameter $-\left(\tilde{I}\left(\frac{L}{\tilde{T}_0}\right) + \tilde{T}_0\partial_t \tilde{I}\left(\frac{L}{t}\right)\Big|_{t=\tilde{T}_0}\right)^{-1}$ (which can be checked to be positive as needed to define a Gumbel distribution). Combining the above calculations we conclude that for the SSRW

$$\begin{aligned} \mathbb{E}^{\text{Asy}}\left[\widetilde{\text{Min}}_L^N\right] &\approx \tilde{T}_0, \\ \text{Var}^{\text{Asy}}\left(\widetilde{\text{Min}}_L^N\right) &\approx \frac{\pi^2}{6\left(\tilde{I}\left(\frac{L}{\tilde{T}_0}\right) + \tilde{T}_0\partial_t \tilde{I}\left(\frac{L}{t}\right)\Big|_{t=\tilde{T}_0}\right)^2}. \end{aligned} \quad (43)$$

Notice that we have dropped the lower order term $\gamma\left(\tilde{I}\left(\frac{L}{\tilde{T}_0}\right) + \tilde{T}_0\partial_t \tilde{I}\left(\frac{L}{t}\right)\Big|_{t=\tilde{T}_0}\right)^{-1}$ from the approximation to $\mathbb{E}^{\text{Asy}}\left[\widetilde{\text{Min}}_L^N\right]$ above, just as we did in the RWRE case. In the limit $L \gg \ln(N)$ we also have $\tilde{T}_0 \gg L$. Thus, using the expansion $\tilde{I}(v) \approx v^2/2$ as $v \rightarrow 0$ we can solve for \tilde{T}_0 and thus extract the following asymptotics, valid

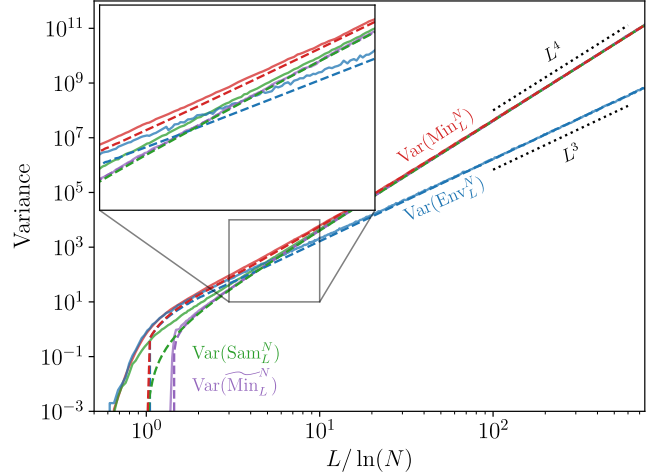


FIG. 4. For the RWRE model with $N = 10^{12}$ particles, we plot we plot the numerically measured (solid) and asymptotic theory (dashed) variance of the extreme first passage time $\text{Var}(\text{Min}_L^N)$ (red); the variance due to the environment $\text{Var}(\text{Env}_L^N)$ (blue); the variance due to sampling $\text{Var}(\text{Sam}_L^N)$ (green). For the SSRW model we plot $\text{Var}(\widetilde{\text{Min}}_L^N)$ (purple).

in the $L \gg \ln(N)$ limit:

$$\begin{aligned} \mathbb{E}^{\text{Asy}}\left[\widetilde{\text{Min}}_L^N\right] &\approx \frac{L^2}{2\ln(N)}, \\ \text{Var}^{\text{Asy}}\left(\widetilde{\text{Min}}_L^N\right) &\approx \frac{\pi^2}{24} \frac{L^4}{(\ln(N))^4}. \end{aligned} \quad (44)$$

These match the corresponding asymptotic sampling mean and variance formulas for the RWRE in Eq. 36.

One-sided case: The same argument and result follows.

VI. COMPARISON OF ASYMPTOTIC AND NUMERICAL RESULTS

We find excellent agreement between our asymptotic theory and numerical simulations not only for very large N , but even for as few as $N = 100$ particles. These results are summarized through a number of figures. As a convention we use solid curves (or data points in Figures 7 and 8) to record outcomes of numerical simulations, dashed curves to record our asymptotic theory, and dotted lines to denote relevant power-laws. All plots are in log-log coordinates so power-laws are straight lines. In Figures 3,5, 6, 7 and 8 each color corresponds to a different value of N while in Figure 4 a single value of N is taken and the colors correspond to numerical and asymptotic curves for the variance of Min_L^N , Env_L^N or Sam_L^N .

Figure 2 shows how we stitch together in Eq. 26 the medium and large distance regimes to produce $\text{Var}^{\text{Asy}}(\text{Env}_L^N)$. It shows that this interpolation scheme provides a smooth crossover between the two regimes and agrees with numerical measurements.

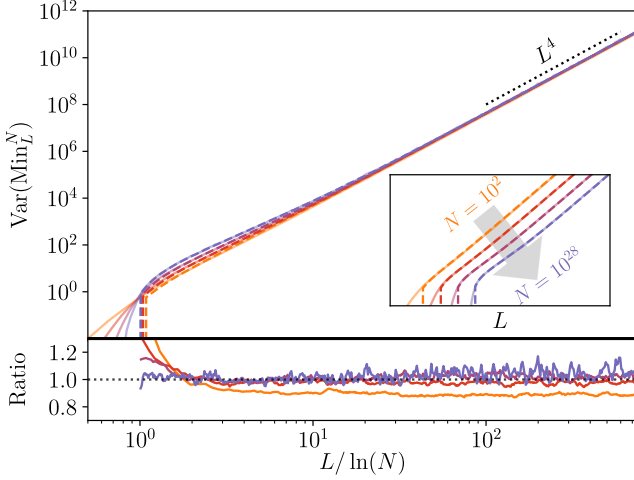


FIG. 5. We plot the numerically measures (solid) and asymptotic theory (dashed) variance of extreme first passage time, $\text{Var}(\text{Min}_L^N)$, for $N = 10^2, 10^5, 10^{12}$ and 10^{28} (each labeled with a different color). The asymptotic theory variance, $\text{Var}^{\text{Asy}}(\text{Min}_L^N)$, comes from Eq. 38. The inset shows the same data uncollapsed to better distinguish different N . The lower plot shows the ratio $\text{Var}^{\text{Num}}(\text{Min}_L^N)/\text{Var}^{\text{Asy}}(\text{Min}_L^N)$.

Figure 3 shows the comparison of the numerical measurements and asymptotic theory for the mean of the extreme first passage time Min_L^N for various N . For system sizes ranging from $N = 10^2$ to 10^{28} the data and asymptotic curves are nearly indistinguishable and fall onto the same master curve given by Eq. 39. The ratio of $\mathbb{E}^{\text{Num}}[\text{Min}_L^N]/\mathbb{E}^{\text{Asy}}[\text{Min}_L^N]$ is nearly 1 for every N indicating the numerics and asymptotic predictions are in agreement. The region with power-law L corresponds to the short distance ballistic regime while the L^2 power-law is valid for all times from the medium distance regime on.

Figure 4 shows the numerical measurements and asymptotic theory for the variance of $\text{Min}_L^N, \text{Sam}_L^N$ and Env_L^N . The theory closely matches the numerical results except for L very close to $\ln(N)$. Presumably, this is due to the finite system size and could be partially remedied by studying the crossover from the short to medium distance regime, for instance using the central limit theorem. In the medium distance regime, the numerical data $\text{Var}^{\text{Num}}(\text{Min}_L^N)$ closely matches $\text{Var}^{\text{Num}}(\text{Env}_L^N)$ as well as the asymptotic formula $\text{Var}^{\text{Asy}}(\text{Env}_L^N)$. In the large distance regime, $\text{Var}^{\text{Num}}(\text{Min}_L^N)$ now closely matches $\text{Var}^{\text{Num}}(\text{Sam}_L^N)$ as well as the asymptotic formula $\text{Var}^{\text{Asy}}(\text{Sam}_L^N)$. This is because in the medium distance regime $\text{Var}(\text{Sam}_L^N) \ll \text{Var}(\text{Env}_L^N)$ while in the large distance regime $\text{Var}(\text{Sam}_L^N) \gg \text{Var}(\text{Env}_L^N)$. The interpolation curve $\text{Var}^{\text{Asy}}(\text{Min}_L^N)$ closely matches $\text{Var}^{\text{Num}}(\text{Min}_L^N)$ over the full medium and long distance regime. For the SSRW, $\text{Var}^{\text{Num}}(\widetilde{\text{Min}}_L^N)$ closely agrees

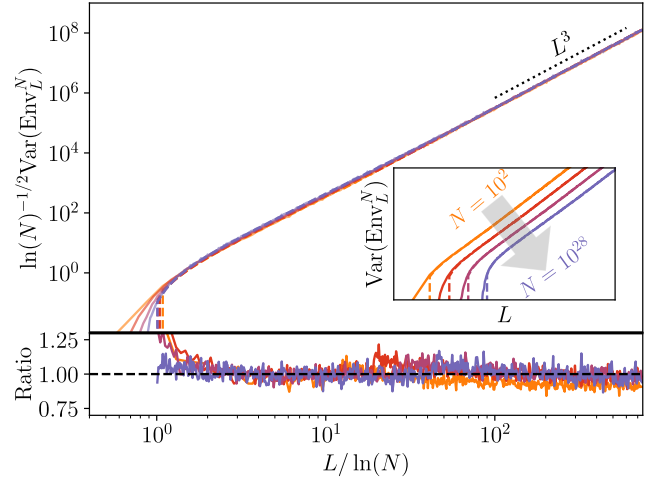


FIG. 6. We plot the numerically measures (solid) and asymptotic theory (dashed) environmental variance, $\text{Var}(\text{Env}_L^N)$, for $N = 10^2, 10^5, 10^{12}$ and 10^{28} (each labeled with a different color). The asymptotic theory variance, $\text{Var}^{\text{Asy}}(\text{Env}_L^N)$, comes from Eq. 26. The inset shows the same data uncollapsed to better distinguish different N . The lower plot shows the ratio $\text{Var}^{\text{Num}}(\text{Env}_L^N)/\text{Var}^{\text{Asy}}(\text{Env}_L^N)$.

with $\text{Var}^{\text{Asy}}(\widetilde{\text{Min}}_L^N)$ (which, as noted earlier, is quite close to $\text{Var}^{\text{Asy}}(\text{Sam}_L^N)$ from the RWRE model for L beyond the medium distance regime.

Figure 5 and 6 show the numerically measured variances of Min_L^N and Env_L^N for a range of system sizes as well as the corresponding asymptotic theory results given by Eqns. 38 and 26, respectively. For large distances, the asymptotic predictions and numerical results match for all system sizes, ranging from $N = 10^2$ to 10^{28} . For $L/\ln(N) \approx 1$ we see additional variance due to finite size effects blunting the transition between the ballistic and diffusive regimes. The ratio of numerics to asymptotic predictions for Min_L^N and Env_L^N are nearly 1 for large $L/\ln(N)$ indicating a good agreement between the numerics and asymptotic predictions. The asymptotic ratio approaches 1 for larger N . However, even for $N = 10^2$ the asymptotic ratio is about .9.

The close agreement between $\text{Var}^{\text{Num}}(\text{Min}_L^N)$ and $\text{Var}^{\text{Asy}}(\text{Min}_L^N)$ in Figure 5 provides a verification of the theoretical addition law, Eq. 37. Figures 7 and 8 provide further confirmation of the addition law. In particular, Figure 7 shows that the numerically measured difference $\text{Var}^{\text{Num}}(\text{Min}_L^N) - \text{Var}^{\text{Num}}(\text{Sam}_L^N)$ follows the asymptotic theory curve $\text{Var}^{\text{Asy}}(\text{Env}_L^N)$. The power-law is clearly recovered, though there is considerably more variation in the ratio of $(\text{Var}^{\text{Num}}(\text{Min}_L^N) - \text{Var}^{\text{Num}}(\text{Sam}_L^N))/\text{Var}^{\text{Asy}}(\text{Env}_L^N)$ than in similar ratios observed in previous figures. This is not so surprising since the difference of two numerical measures introduces additional error. Also for larger N , the number of systems used to estimate the variances is smaller than for

small N , thus introducing additional error for large N .

Figure 8 shows another route to measure the environmental variance $\text{Var}(\text{Env}_L^N)$ by taking the difference $\text{Var}^{\text{Num}}(\text{Min}_L^N) - \text{Var}^{\text{Asy}}(\widetilde{\text{Min}}_L^N)$. As we explain in Section VII, we use $\text{Var}^{\text{Asy}}(\widetilde{\text{Min}}_L^N)$ instead of $\text{Var}^{\text{Asy}}(\text{Sam}_L^N)$ here since in experimental settings it may be possible to estimate the Einstein diffusion coefficient and hence develop a prediction for $\text{Var}^{\text{Asy}}(\widetilde{\text{Min}}_L^N)$. Since we have shown above that $\text{Var}^{\text{Asy}}(\widetilde{\text{Min}}_L^N)$ and $\text{Var}^{\text{Asy}}(\text{Sam}_L^N)$ match beyond the medium distance regime, we thus expect to still be able to recover the power-law behavior of $\text{Var}(\text{Env}_L^N)$ by studying $\text{Var}^{\text{Num}}(\text{Min}_L^N) - \text{Var}^{\text{Asy}}(\widetilde{\text{Min}}_L^N)$.

In Figure 8, the dots record positive values of this difference $\text{Var}^{\text{Num}}(\text{Min}_L^N) - \text{Var}^{\text{Asy}}(\widetilde{\text{Min}}_L^N)$ (scaled by $(\ln(N))^{1/2}$, as one should to see a collapse of the data) and the \times records the magnitude of negative values of this difference. Clearly, the presence of negative values contradicts the addition law and recovery of $\text{Var}(\text{Env}_L^N)$. These values, however, only arise for either small N (10^2 and 10^5) or large L . For large N (10^{12} and 10^{28}) the dots closely follow the asymptotic environmental variance curve $\text{Var}^{\text{Asy}}(\text{Env}_L^N)$ for just under two decades (as evidenced from the ratio being close to 1) and then peel off following what looks to be an L^4 power-law (as opposed to the L^3 power-law behavior of $\text{Var}^{\text{Asy}}(\text{Env}_L^N)$). The explanation for the lack of agreement for small N or large L likely arises from the presence of higher order corrections to $\text{Var}^{\text{Asy}}(\widetilde{\text{Min}}_L^N)$ which scale like L^4 but with pre-factors that decay with N (the presence of such terms can be seen from [67]). Therefore, for small N or large L these corrections become relevant.

VII. CONCLUSION

We consider two models for many-particle diffusion in a common environment. The first treats each particle as an independent SSRW while the second RWRE model treats the environment as a space-time random biasing field within which each particle performs biased random walks. We focus on the extreme first passage time Min_L^N , i.e., the time when the first of N particles passes a barrier distance L from their common starting location. We show that the randomness of Min_L^N splits into two essentially independent pieces, the randomness Env_L^N from the environment and the randomness Sam_L^N from sampling N random walks within that environment.

We determine theoretical predictions (related to the

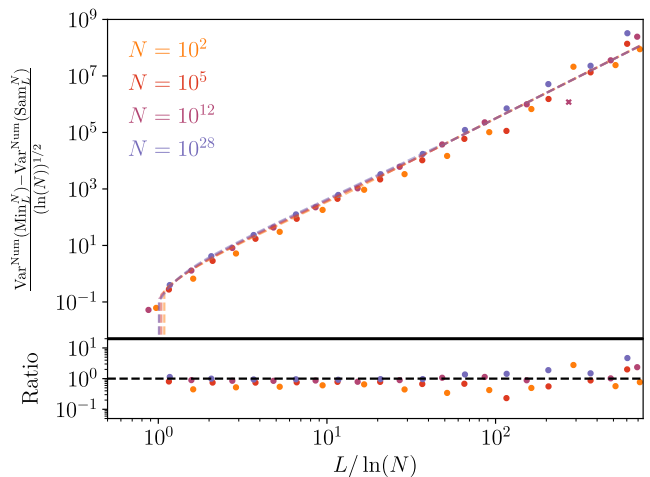


FIG. 7. We plot $\text{Var}^{\text{Num}}(\text{Min}_L^N) - \text{Var}^{\text{Num}}(\text{Sam}_L^N)$ for $N = 10^2, 10^5, 10^{12}$ and 10^{28} averaged over each horizontal 1/4 decade. The dashed line is $\text{Var}^{\text{Asy}}(\text{Env}_L^N)$ in Eq. 26 for each N corresponding to its respective color.

KPZ universality class and equation) for the behavior of each of these contributions based on asymptotic limit theorems in different scaling regimes of N and L . While $\text{Var}(\text{Sam}_L^N)$ closely matches the variance from sampling in the SSRW model for large L , the $\text{Var}(\text{Env}_L^N)$ term has no parallel in the SSRW case where the environment is deterministic. We uncover a novel $L^3/(\ln(N))^{5/2}$ power-law describing the large L behavior of $\text{Var}(\text{Env}_L^N)$. This should be contrasted with the $L^4/(\ln(N))^4$ power-law that we demonstrate describes the large L behavior of $\text{Var}(\text{Sam}_L^N)$. Thus, for large L , owing to the independence of Env_L^N and Sam_L^N , we see that $\text{Var}(\text{Min}_L^N) = \text{Var}(\text{Env}_L^N) + \text{Var}(\text{Sam}_L^N)$ and only the L^4 power-law is visible. We numerically verify all of our predictions for system sizes ranging from $N = 10^2$ to $N = 10^{28}$ and, remarkably, see close agreement over this entire range.

Our results point to a potential experimental approach to probe the nature of a random or disordered environment by observing the extreme behavior of many particles diffusing within it. In Figure 8 we show that it is possible to recover, over multiple decades, the L^3 power-law behavior of $\text{Var}(\text{Env}_L^N)$ by numerically measuring $\text{Var}(\text{Min}_L^N)$ and then subtracting the asymptotic theory formula for $\text{Var}(\widetilde{\text{Min}}_L^N)$, the SSRW extreme first passage time variance. This is because the asymptotic behavior of $\text{Var}(\widetilde{\text{Min}}_L^N)$ for $L \gg \ln(N)$ essentially matches that of $\text{Var}(\text{Sam}_L^N)$ in the RWRE model. For the SSRW model (or its Brownian analog), a formula for $\text{Var}(\text{Min}_L^N)$ can be determined asymptotically just by knowing the Einstein diffusion coefficient, which in turn can be estimated experimentally by following the motion of a single particle. Thus, by observing the motion

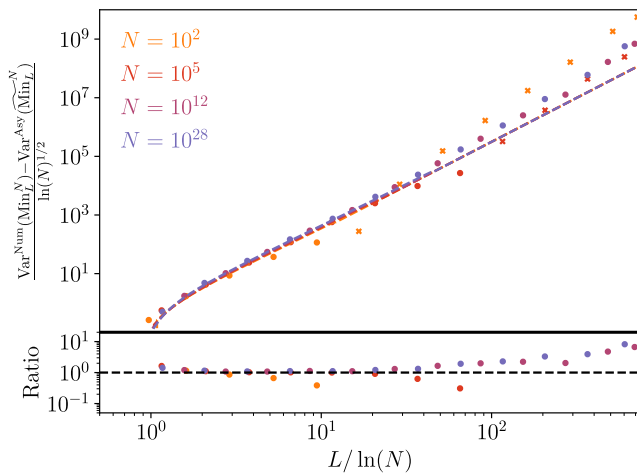


FIG. 8. We plot $\text{Var}^{\text{Num}}(\text{Min}_L^N) - \text{Var}^{\text{Asy}}(\widetilde{\text{Min}}_L^N)$ for $N = 10^2, 10^5, 10^{12}$ and 10^{28} , averaged over each horizontal 1/4 decade. The dots represent positive values of this difference whereas the \times represents the magnitude of negative values of this difference. The dashed line is $\text{Var}^{\text{Asy}}(\text{Env}_L^N)$ in Eq. 26 for each N corresponding to its respective color.

(i.e., extreme first passage time, and Einstein diffusion coefficient) of many particles diffusing in a common environment we are (at least in our numerical simulations) able to recover the power-law that describes the environmental fluctuations. Moreover, with some error, we are also able to estimate the pre-factor of this power-law, which contains further information about the random environment. This pre-factor could be termed the *extreme diffusion coefficient* and in future work we plan to develop a more general map between random environments (beyond the special Uniform on $[0, 1]$ choice) and extreme diffusion coefficients.

In experimental systems such as N colloids or fluorescent dyes diffusing in quasi-1D channels, or photons (here N relates to the laser intensity) diffusing through a quasi-1D tubes filled with scattering media, it should be possible to precisely observe first passage times to various distances, as well as to estimate the Einstein diffusion coefficient for a single particle. Our numerical conclusions suggest a possible route to observe the hidden environment within which these real diffusions occur. Uncovering an L^3 power-law would strongly suggest that the RWRE model more accurately captures the behavior of extreme behavior in many particle diffusions. Moreover, the pre-factor to this power-law would constitute a measurement of the *extreme diffusion coefficient* and thus serve as a microscope through which to view the hidden environment.

VIII. ACKNOWLEDGMENTS

This work was funded under the W.M. Keck Foundation Science and Engineering grant on “Extreme Diffusion”. I.C. also wishes to acknowledge ongoing support from the NSF through DMS:1811143, DMS:1937254, and DMS:2246576, and the Simons Foundation through a Simons Investigator Grant (Award ID 929852). E.I.C. wishes to acknowledge ongoing support from the Simons Foundation for the collaboration Cracking the Glass Problem via Award No. 454939. We wish to thank S. Prolhac for providing data for the numerically computed density of the one-point distribution for the narrow wedge solution to the KPZ equation that was utilized in producing some of the asymptotic curves herein. We also wish to thank P. Le Doussal for helpful comments on a draft of this paper. This work benefited from access to the University of Oregon high performance computing cluster, Talapas.

-
- [1] Baruch Meerson and S. Redner. Mortality, Redundancy, and Diversity in Stochastic Search. *Physical Review Letters*, 114(19):198101, May 2015.
 - [2] Z. Schuss, K. Basnayake, and D. Holcman. Redundancy principle and the role of extreme statistics in molecular and cellular biology. *Physics of Life Reviews*, 28:52–79, March 2019.
 - [3] J. Yang, I. Kupka, Z. Schuss, and D. Holcman. Search for a small egg by spermatozoa in restricted geometries. *Journal of Mathematical Biology*, 73:423–446, 2016.
 - [4] Kanishka Basnayake, David Mazaud, Alexis Bemelmans, Nathalie Rouach, Eduard Korkotian, and David Holcman. Fast calcium transients in dendritic spines driven by extreme statistics. *PLOS Biology*, 17(6):e2006202, June 2019.
 - [5] Renato Germano and Alessandro P. S. de Moura. Traffic of particles in complex networks. *Physical Review E*, 74(3):036117, September 2006.
 - [6] Shao-Ping Wang and Wen-Jiang Pei. First passage time of multiple Brownian particles on networks with applications. *Physica A: Statistical Mechanics and its Applications*, 387(18):4699–4708, July 2008.
 - [7] A. Einstein. Zur Theorie der Brownschen Bewegung. *Annalen der Physik*, 324(2):371–381, January 1906.
 - [8] A. Einstein. über die von der molekularkinetischen Theorie der Wärme geforderte Bewegung von in ruhenden Flüssigkeiten suspendierten Teilchen. *Annalen der Physik*, 322(8):549–560, 1905.
 - [9] A. Einstein. Theoretische Bemerkungen Über die Brownsche Bewegung. *Zeitschrift für Elektrochemie und angewandte physikalische Chemie*, 13(6):41–42, February 1907.
 - [10] Sidney Redner. *A Guide to First-Passage Processes*. Cambridge University Press, Cambridge, 2001.
 - [11] Samantha Linn and Sean D. Lawley. Extreme hitting probabilities for diffusion. *Journal of Physics A: Mathematical and Theoretical*, 55(34):345002, August 2022.

- [12] S. Redner and B. Meerson. Redundancy, extreme statistics and geometrical optics of Brownian motion: Comment on “Redundancy principle and the role of extreme statistics in molecular and cellular biology” by Z. Schuss et al. *Physics of Life Reviews*, 28:80–82, March 2019.
- [13] Sean D. Lawley. Distribution of extreme first passage times of diffusion. *Journal of Mathematical Biology*, 80(7):2301–2325, June 2020.
- [14] Katja Lindenberg, V. Seshadri, K. E. Shuler, and George H. Weiss. Lattice random walks for sets of random walkers. First passage times. *Journal of Statistical Physics*, 23(1):11–25, July 1980.
- [15] Jacob B. Madrid and Sean D. Lawley. Competition between slow and fast regimes for extreme first passage times of diffusion. *Journal of Physics A: Mathematical and Theoretical*, 53(33):335002, July 2020.
- [16] Denis S. Grebenkov, Ralf Metzler, and Gleb Oshanin. From single-particle stochastic kinetics to macroscopic reaction rates: Fastest first-passage time of N random walkers. *New Journal of Physics*, 22(10):103004, October 2020.
- [17] Sean D. Lawley. Universal formula for extreme first passage statistics of diffusion. *Physical Review E*, 101(1):012413, January 2020.
- [18] F. Rassoul-Agha and T. Seppäläinen. An almost sure invariance principle for random walks in a space-time random environment. *Probability Theory and Related Fields*, 133(3):299–314, November 2005.
- [19] Jean-Dominique Deuschel, Xiaoqin Guo, and Alejandro F. Ramírez. Quenched invariance principle for random walk in time-dependent balanced random environment. *Annales de l’Institut Henri Poincaré, Probabilités et Statistiques*, 54(1):363–384, February 2018.
- [20] Firas Rassoul-Agha, Timo Seppäläinen, and Atilla Yilmaz. Quenched Free Energy and Large Deviations for Random Walks in Random Potentials. *Communications on Pure and Applied Mathematics*, 66(2):202–244, 2013.
- [21] Guillaume Barraquand and Ivan Corwin. Random-walk in Beta-distributed random environment. *Probability Theory and Related Fields*, 167(3-4):1057–1116, April 2017.
- [22] Guillaume Barraquand and Pierre Le Doussal. Moderate deviations for diffusion in time dependent random media. *Journal of Physics A: Mathematical and Theoretical*, 53(21):215002, May 2020.
- [23] Jacob B. Hass, Aileen N. Carroll-Godfrey, Ivan Corwin, and Eric I. Corwin. Anomalous fluctuations of extremes in many-particle diffusion. *Physical Review E*, 107(2):L022101, February 2023.
- [24] Thimothée Thiery and Pierre Le Doussal. Exact solution for a random walk in a time-dependent 1D random environment: The point-to-point Beta polymer. *Journal of Physics A: Mathematical and Theoretical*, 50(4):045001, December 2016.
- [25] Ivan Corwin and Yu Gu. Kardar–Parisi–Zhang Equation and Large Deviations for Random Walks in Weak Random Environments. *Journal of Statistical Physics*, 166(1):150–168, January 2017.
- [26] Pierre Le Doussal and Thimothée Thiery. Diffusion in time-dependent random media and the Kardar–Parisi–Zhang equation. *Physical Review E*, 96(1):010102, July 2017.
- [27] Guillaume Barraquand and Mark Rychnovsky. Large deviations for sticky Brownian motions. *Electronic Journal of Probability*, 25:1–52, January 2020.
- [28] Guillaume Barraquand and Mark Rychnovsky. Random Walk on Nonnegative Integers in Beta Distributed Random Environment. *Communications in Mathematical Physics*, 398(2):823–875, March 2023.
- [29] Dom Brockington and Jon Warren. The Bethe ansatz for sticky Brownian motions. *Stochastic Processes and their Applications*, 162:1–48, August 2023.
- [30] Dom Brockington and Jon Warren. At the edge of a cloud of Brownian particles. *arXiv:2208.11952 [math]*, August 2022.
- [31] Giancarlos Oviedo, Gonzalo Panizo, and Alejandro F. Ramírez. Second order cubic corrections of large deviations for perturbed random walks. *Electronic Journal of Probability*, 27:1–45, January 2022.
- [32] Sayan Das, Hindy Drillick, and Shalin Parekh. KPZ equation limit of sticky Brownian motion. *arXiv.2304.14279 [math]*, April 2023.
- [33] Alexander K. Hartmann, Alexandre Krajenbrink, and Pierre Le Doussal. Probing the large deviations for the Beta random walk in random medium. *arXiv:2307.15041 [cond-mat]*, July 2023.
- [34] Alexandre Krajenbrink and Pierre Le Doussal. The crossover from the Macroscopic Fluctuation Theory to the Kardar-Parisi-Zhang equation controls the large deviations beyond Einstein’s diffusion. *Physical Review E*, 107(1):014137, January 2023.
- [35] Bo Wang, James Kuo, Sung Chul Bae, and Steve Granick. When Brownian diffusion is not Gaussian. *Nature Materials*, 11(6):481–485, May 2012.
- [36] Ralf Metzler. Brownian motion and beyond: First-passage, power spectrum, non-Gaussianity, and anomalous diffusion. *Journal of Statistical Mechanics: Theory and Experiment*, 2019(11):114003–114003, November 2019.
- [37] Jean-Philippe Bouchaud and Antoine Georges. Anomalous diffusion in disordered media: Statistical mechanisms, models and physical applications. *Physics Reports*, 195(4):127–293, November 1990.
- [38] Sriram Ramaswamy. The Mechanics and Statistics of Active Matter. *Annual Review of Condensed Matter Physics*, 1(1):323–345, 2010.
- [39] Kiyoshi Kanazawa, Tomohiko G. Sano, Andrea Cairoli, and Adrian Baule. Loopy Lévy flights enhance tracer diffusion in active suspensions. *Nature*, 579(7799):364–367, March 2020.
- [40] Lewis Fry Richardson and Gilbert Thomas Walker. Atmospheric diffusion shown on a distance-neighbour graph. *Proceedings of the Royal Society of London. Series A, Containing Papers of a Mathematical and Physical Character*, 110(756):709–737, April 1926.
- [41] H. G. E. Hentschel and Itamar Procaccia. Relative diffusion in turbulent media: The fractal dimension of clouds. *Physical Review A*, 29(3):1461–1470, March 1984.
- [42] J. P. Bouchaud. Diffusion and Localization of Waves in a Time-Varying Random Environment. *Europhysics Letters (EPL)*, 11(6):505–510, March 1990.
- [43] M. Chertkov and G. Falkovich. Anomalous Scaling Exponents of a White-Advection Passive Scalar. *Physical Review Letters*, 76(15):2706–2709, April 1996.
- [44] Denis Bernard, Krzysztof Gawędzki, and Antti Kupiainen. Anomalous Scaling in the N -Point Functions of Passive Scalar. *Physical Review E*, 54(3):2564–2572, September 1996.

- [45] H. Kesten, M. V. Kozlov, and F. Spitzer. A limit law for random walk in a random environment. *Compositio Mathematica*, 30(2):145–168, 1975.
- [46] Y. Sinai. The Limiting Behavior of a One-Dimensional Random Walk in a Random Medium. *Theory of Probability & Its Applications*, 27(2):256–268, January 1983.
- [47] J. P. Bouchaud, A. Comtet, A. Georges, and P. Le Doussal. Classical diffusion of a particle in a one-dimensional random force field. *Annals of Physics*, 201(2):285–341, August 1990.
- [48] S. F. Burlatsky and John M. Deutch. Transient relaxation of a charged polymer chain subject to an external field in a random tube. *The Journal of Chemical Physics*, 109(6):2572–2578, August 1998.
- [49] A. A. Chernov. Replication of a multicomponent chain by the “lightning” mechanism. *Biophysics*, 12(2), 1967.
- [50] D. E. Temkin. One-dimensional random walks in a two-component chain. *Soviet Math. Docl.*, 13:1172–1176, 1972.
- [51] Barry D. Hughes. *Random Walks and Random Environments: Random Walks*. Clarendon Press, 1995.
- [52] Zeitouni Ofer. Random walks in random environment. In *Lectures on Probability Theory and Statistics, Lecture Notes*, volume 1837 of *Math*, pages 189–312. Springer, Berlin, 2004.
- [53] Pierre Le Doussal. First-passage time for random walks in random environments. *Physical Review Letters*, 62(26):3097–3097, June 1989.
- [54] S. H. Noskowitz and I. Goldhirsch. Average versus Typical Mean First-Passage Time in a Random Random Walk. *Physical Review Letters*, 61(5):500–502, August 1988.
- [55] Pierre Le Doussal and Thimothée Thiery. Diffusion in time-dependent random media and the Kardar-Parisi-Zhang equation. *arXiv:1705.05159 [cond-mat]*, May 2017.
- [56] Craig A. Tracy and Harold Widom. Level-spacing distributions and the Airy kernel. *Communications in Mathematical Physics*, 159(1):151–174, January 1994.
- [57] Mehran Kardar, Giorgio Parisi, and Yi-Cheng Zhang. Dynamic Scaling of Growing Interfaces. *Physical Review Letters*, 56(9):889–892, March 1986.
- [58] Tomohiro Sasamoto and Herbert Spohn. One-Dimensional Kardar-Parisi-Zhang Equation: An Exact Solution and its Universality. *Physical Review Letters*, 104(23):230602, June 2010.
- [59] P. Calabrese, P. Le Doussal, and A. Rosso. Free-energy distribution of the directed polymer at high temperature. *EPL (Europhysics Letters)*, 90(2):20002, April 2010.
- [60] V. Dotsenko. Bethe ansatz derivation of the Tracy-Widom distribution for one-dimensional directed polymers. *EPL (Europhysics Letters)*, 90(2):20003, April 2010.
- [61] Gideon Amir, Ivan Corwin, and Jeremy Quastel. Probability Distribution of the Free Energy of the Continuum Directed Random Polymer in 1+1 dimensions. *Communications on Pure and Applied Mathematics*, 64(4):466–537, April 2011.
- [62] Ivan Corwin. The kardar-parisi-zhang equation and universality class. *Random Matrices: Theory and Applications*, 01(01):1130001, January 2012.
- [63] Jeremy Quastel and Herbert Spohn. The One-Dimensional KPZ Equation and Its Universality Class. *Journal of Statistical Physics*, 160(4):965–984, August 2015.
- [64] Konstantin Matetski, Jeremy Quastel, and Daniel Remenik. The KPZ fixed point. *Acta Mathematica*, 227(1):115–203, September 2021.
- [65] Sylvain Prolhac. Personal Communication, February 2022.
- [66] Sylvain Prolhac and Herbert Spohn. The height distribution of the KPZ equation with sharp wedge initial condition: Numerical evaluations. *Physical Review E*, 84(1):011119, July 2011.
- [67] Lior Zarfaty, Eli Barkai, and David A. Kessler. Accurately approximating extreme value statistics. *Journal of Physics A: Mathematical and Theoretical*, 54(31):315205, July 2021.